Transport Processes in the Atmosphere Leading to Radioactive Fallout

By
Elmar R. Reiter

Progress Report No. 1; September 1964
Contract No. AT(11-1)-1360
With U.S. Atomic Energy Commission

Technical Paper No. 58
Department of Atmospheric Science
Colorado State University
Fort Collins, Colorado

Colorado State University

Department of Atmospheric Science

Paper No. 58

TRANSPORT PROCESSES IN THE ATMOSPHERE LEADING TO RADIOACTIVE FALLOUT

Progress Report No. 1
Contract No. AT(11-1) - 1360
with U.S. ATOMIC ENERGY COMMISSION

Project Leader
Elmar R. Reiter

Colorado State University
Department of Atmospheric Science
Technical Paper No. 58

September 1964

TABLE OF CONTENTS

Page

Relation of Stratospheric-Tropospheric Mass Exchange Mechanisms to Surface Radioactivity Peaks;
by J. D. Mahlman 1

Heavy Radioactive Fallout Over the Southern United States, November 1962;
by Elmar R. Reiter and J. D. Mahlman 21

Debris Source of The Heavy Fallout Over Southern United States on 24-27 November 1962;
by J. D. Mahlman and William E. Davis 51

On The Feasibility of Relating Seasonal Fallout Oscillations to Hemispheric Index Patterns;
by J. D. Mahlman 55

RELATION OF STRATOSPHERIC-TROPOSPHERIC MASS EXCHANGE MECHANISMS TO SURFACE RADIOACTIVITY PEAKS

by

J. D. Mahlman

ABSTRACT

The atmospheric origin of an area of sudden increase of surface radioactivity is studied. Because all the radioactivity measurements show the mean debris ages to be greater than one hundred days for the entire sequence, the air is inferred to have been of recent stratospheric origin in view of an assumed mean tropospheric debris residence time of one month.

The trajectories of the layer which caused the sudden increase in debris concentration were traced isentropically backward from the point of the fallout increase. The computed trajectory is traced backward to the region traditionally considered to be the "jet stream front" and is shown definitely to be stratospheric air through potential vorticity considerations. The sinking motion is seen to be associated with upper air cyclogenesis and takes place to the rear of the high level cyclone. The air appears to cross the jet axis as viewed on an isobaric surface; but viewed isentropically, the trajectory is seen to "slip under" the jet core in such manner that no appreciable lateral shears are observed.

I. INTRODUCTION

The phenomenon of seasonal variations in radioactive fallout has received considerable attention since the initial observations of it in the middle 1950's. Especially interesting aspects of this are the sudden increases of surface radioactivity intensity which often have been observed (Reiter, 1963b). This has been noted to occur most often in the spring resulting in a mean radioactivity maximum at this time of year.

Purpose

The purpose of this research is to trace isentropic trajectories backward from an observed fallout maximum in order to determine its immediate atmospheric origin. Thus the hypothesis that the descent of mass and radioactivity from the stratosphere is associated with high level extratropical cyclones will be further tested (Staley, 1960, 1962).

Literature Pertaining to the Problem

A great wealth of literature exists which pertains directly or indirectly to seasonal and latitudinal surface radioactive fallout variations and their subsequent physical interpretations. For some time it was not clear as to whether or not seasonal and latitudinal fallout maxima even existed. Because of the large amount of research and work in this field, it is now possible to evaluate the reality of their existence.

Soon after the initial extensive thermonuclear testing took place, it was established that surface radioactive debris, measured some time after atmospheric testing took place, was predominately of stratospheric origin.[1] This inference was reached by calculating ratios of strontium-89 and strontium-90 and thus estimating the debris age by the rate of depletion of strontium-89 relative to strontium-90 (half-life of strontium-89 = 50.5 days; half-life of strontium-90 = 27.7 years). Implicit in these measurements was the assumption that the mean tropospheric debris residence time was of the order of one month. Thus, proceeding from this postulate, any debris whose age is shown by use of strontium-89, strontium-90 ratios to be considerably greater than one month is alleged to be of stratospheric origin.

Naturally the mean stratospheric residence times would be somewhat longer because of the higher static stabilities and lack of precipitation scavenging in this region. For example one of the first publications on this subject estimated that the mean stratospheric debris residence time was of the order of five to ten years (Libby, 1956). In arriving at this figure Libby assumed that the debris would be uniformly mixed throughout the stratosphere shortly after detonation. He then stated that the debris probably enters the stratosphere by uniform mixing and consequently is directly and highly correlated with rainfall areas. However, Machta and List (1959) showed by actual flight measurements that debris concentrations in the stratosphere are extremely variable. They also gave a mean residence time of less than five years. However, they acknowledged that the model is far too simple and needs to take into account the differences in residence time with latitude and altitude. As a result of later investigations, Libby (1959) revised his earlier estimate to a residence time of five years for debris in the equatorial stratosphere and one year or less in the polar stratosphere. In light of present evidence this latter estimate seems to be the most reasonable.

Prior to the 1960's radioactivity measurements were taken only at isolated locations on the earth, so that the conclusions drawn from them could conceivably lack generality as far as the entire globe is concerned. This is especially so, if it is found that the stratospheric debris is not mixed uniformly into the troposphere. For example, it is conceivable that the debris could enter the troposphere by discrete intrusions in a completely non-uniform manner (Staley, 1960). However, in spite of this, measurements taken at Milford Haven showed quite well pronounced spring maxima to exist there in 1955, 1956, and 1957.[2] Also the same paper concerning measurements taken in 1956 showed a very strong latitudinal distribution of mean debris concentration that was characterized by a sharp peak at 40° north latitude and a less pronounced maximum at 40° south latitude. However, Martell (1959) interpreted the less pronounced maximum in the southern hemisphere

[1] Stewart, N.G., R.G.D. Osmond, R.N. Crooks, E.M.R. Fisher, and M.J. Owens, 1957: The world wide deposition of long-lived fission products from nuclear explosions, Atomic Energy Research Establishment, HP/R 2790 Harwell.

[2] Machta, L., 1957: Discussion of meteorological factors and fallout distribution, U.S. Department of Commerce, Weather Bureau Publication, 11 pp.

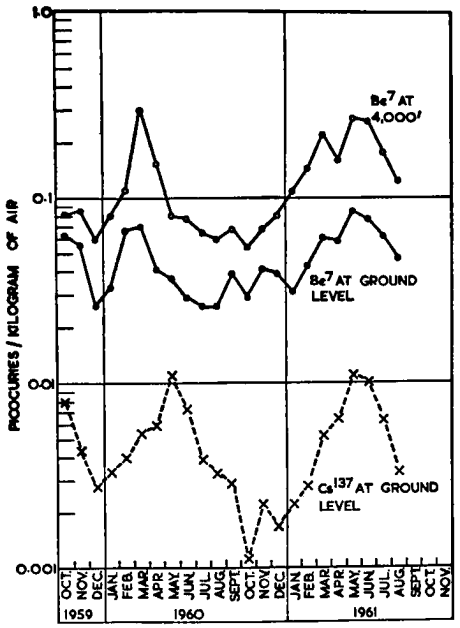

Fig. 1: Seasonal concentration of beryllium-7 and cesium-137 in micro-micro curies (picocuries) per kilogram of air over Great Britain (Peirson, 1963).

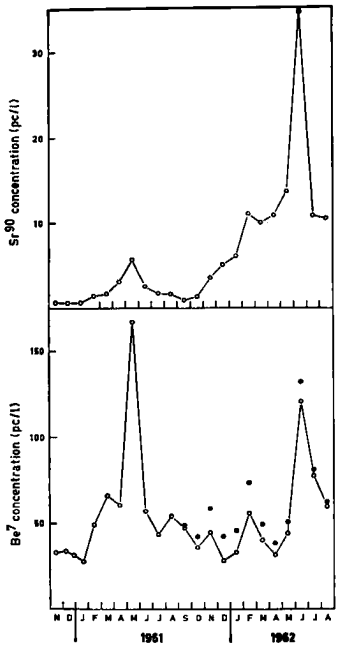

Fig. 2: Seasonal concentration of beryllium-7 and strontium-90 in rain water at Rijswijk, The Netherlands. Total beryllium-7 is represented by solid circles, natural beryllium-7 by open circles (Bleichrodt and Van Abkoude, 1963).

to imply that the northern hemisphere latitudinal maximum was due to preferential injection of debris at the same latitude. Thus he stated that debris injected in the high tropical atmosphere from equatorial tests would not result in a mid-latitude maximum at a later time.

Measurements taken at Rijswijk, The Netherlands, showed statistically significant spring maxima for every year from 1957 to 1960 (Bleichrodt, Blok, and Dekker, 1961; Bleichrodt, Blok, and Van Abkoude, 1961). Because of the wide differences in amplitude of the spring maximum from year to year, it is postulated that the seasonal radioactivity changes are due to a meterological effect, but the amount of debris is proportional to the stratospheric inventory from year to year.

An analysis of stratospherically produced strontium-90 debris for 1959 (Libby and Palmer, 1960) revealed a striking spring peak of debris from the Russian October tests of the previous year. Also a pronounced latitudinal variation was shown with a definite maximum at 35° north latitude. Fry, Jew, and Kuroda (1960) studied the 1959 peak by chemical dating methods and concluded that it contained debris which was older than could be explained by the Russian tests. Measurements taken at Argonne National Laboratory revealed an increase of cesium-137 from April to June 1960, although no nuclear tests were made in the previous year (Gustafson et al., 1961). Analyses of artificially produced tritium showed spring maxima for the years 1958, 1959, and 1960 that are remarkably in phase with the strontium-90 measurements for those years (Libby, 1961). Studies of cesium-137 measurements taken at Rijswijk, The Netherlands, documented spring increases for every year from 1957 to 1960 (Bleichrodt, Blok, and Dekker, 1961; Bleichrodt, Blok, and Van Abkoude, 1961). Measurements taken at two stations for isotopes of beryllium-7 and cesium-137 showed distinct peaks during March 1960 and May 1961 (Peirson, 1963) (Fig. 1).

One of the most interesting studies on this problem (Bleichrodt and Van Abkoude, 1963) was concerned with the intensity of naturally occurring beryllium-7 and its seasonal variations (Fig. 2). A definite seasonal dependence was noted, again characterized by a pronounced maximum in the spring of the year. This is especially significant,

because natural beryllium-7 is only produced in the upper regions of the atmosphere by photochemical means. Hence it may be concluded that the seasonal dependence of this tracer element may definitely be related to seasonal changes in the mechanism of stratospheric-tropospheric mass exchange.

The literature which seriously deals with the mechanism of mass exchange is quite limited. According to Libby (1956), the debris probably enters the troposphere at uniform rates and consequently is removed from the atmosphere by precipitation scavenging processes (Greenfield, 1957; Kruger and Hosler, 1963).

Another explanation of the spring peak is that this time of year is a period of more rapid downward mixing of stratospheric air into the troposphere.[3] By a similar argument, the latitudinal distribution is alleged to be due to a "selective zone of downward mixing at middle latitudes". Martell and Drevinsky (1960) argued that the polar debris is removed from the stratosphere by subsidence or intensified mixing in early spring. They further stated that the large difference in debris concentrations between polar and subtropical rains is due to precipitation scavenging along the polar front.

A study by Miyake et al. (1962), which correlated increases in surface radioactivity with upper air flow patterns, yielded some very interesting results. They discovered that a strong correlation existed between increases of surface radioactivity and a cyclone aloft at 500 millibars. Because of this they hypothesized that the descent of mass from the stratosphere occurs to the rear of high level extratropical cyclones.

In consideration of the "waterspout" model of the upper tropospheric frontal zone (Reed and Danielsen, 1959), it was concluded that "folding" of the tropopause was the mechanism which resulted in the descent of stratospheric air into the troposphere. Later Danielsen (1959) studied the descent of mass from the stratosphere along stable laminae which are shown to persist in space and time. Since his analysis of these stable laminae showed that the tropopause is not a substantial surface which confines air to the stratosphere, it is no longer necessary to resort to the concept of the "folded tropopause" that he proposed earlier. Reiter (1963a, 1963b) considers this type of exchange through the "jet stream front" and corroborates through an actual trajectory analysis the validity of this transport mechanism. It is also postulated (Storebø, 1959) that the exchange might possibly be due to cyclonic eddies relative to the subtropical jet stream, thus creating maximum exchange in late winter. He later altered this stand and suggests that the spring peak is attributable to the breakdown of the polar night vortex in the upper stratosphere (Storebø, 1960). This view also conforms to that of Libby and Palmer (1960).

In a detailed case study by Staley (1960) actual trajectories of air parcels were traced along isentropic surfaces common to both stratosphere and troposphere. The study clearly documented, for this particular case at least, that it is possible to trace parcel trajectories which leave the stratosphere and descent to within a short distance of the earth's surface. This descent is in the same sense as proposed by other authors (Reed and Danielsen, 1959; Danielsen, 1959; Reiter, 1963a, 1963b), but it is further stated that this "waterspout" is associated with extratropical cyclones. If Staley's (1962) hypothesis that the descent occurs in high level cyclones is correct, then it is conceivable that the seasonal variations in surface radioactivity may be directly related to the number and intensity of high level baroclinic extratropical disturbances.

II. THE FALLOUT SITUATION

The mean radioactive fallout pattern over the United States exhibits a strong seasonal variation in intensity when fallout peaks due to fresh atmospheric atomic weapons testing are discounted (Fig. 3). According to Staley (1960), these mean seasonal variations are a result of discrete changes in observed surface fallout intensity throughout the year. It thus is advisable to approach the larger problem of explaining the seasonal fallout variations by first investigating the physical processes which produce such discrete changes in fallout intensity. Because of the atmospheric atomic testing moratorium which began in December 1962, the period following the last tests provides an excellent opportunity for studying variations of long-lived radioactive fallout and the physical basis for these variations.

It appears that the surface fallout in the first half of 1963 contained distinct mean maxima in January and April (Fig. 3). At the end of March a large increase in surface fallout was observed. On 28 and 29 March the surface distribution of

[3] Stewart, loc. cit.

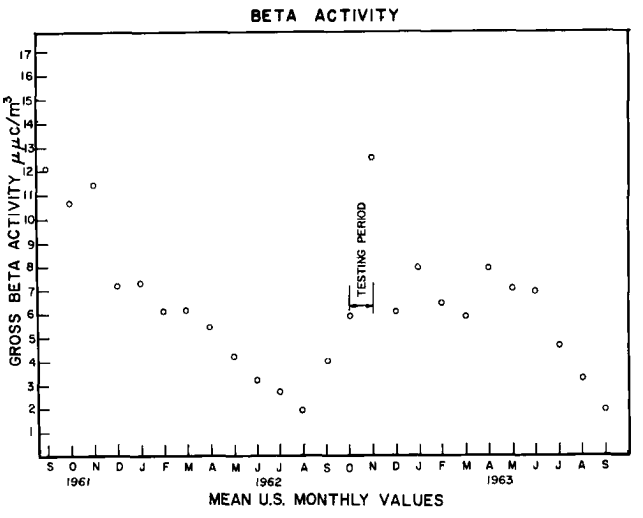

Fig. 3: Time section of mean monthly gross beta radioactivity in air computed by a weighted average of stations over the United States fallout observation network from November 1961 to September 1963. Ordinate is mean radioactivity in micro-micro Curies per cubic meter. All fallout data was obtained from the Public Health Service Surveillance Network.

radioactive products (measured in micro-micro curies per cubic meter) contained no values which were appreciably above the mean intensity for this period (Fig. 4). However, on 30 March the observed intensities in the Colorado, Nebraska, Utah, and Wyoming region were nearly three times as high as those observed on the previous day. On subsequent days this fallout region was associated with weak surface winds and thus showed little movement from its original position (Fig. 4).

This case is exceedingly interesting in view of the fact that no precipitation was observed anywhere in the region for the three day period before, during, and after the sudden fallout increase was noted. Hence, this definitely rules out the possibility of fallout increase due to precipitation scavenging of radioactive particulate matter as proposed by Greenfield (1957). Also of interest is the fact that the debris age is computed to be greater than one hundred days for every United States observing station for the entire sequence. If one recognizes that the mean tropospheric residence time for a radioactive particle is estimated to be of the order of one month, it is readily inferred that the debris is probably of stratospheric origin. That this is reasonable may be expected from the higher static stabilities and hence much longer particle residence times in the stratosphere (Libby, 1956; Libby, 1959; Machta and List, 1959).

III. METHOD OF APPROACH

On the basis of the evidence presented the objective is to trace the movement of the debris and evaluate the mechanism which leads to this sudden increase of surface radioactive fallout. If the debris-carrying air mass originated in the stratosphere, it should display characteristics which would positively identify it. According to Danielsen (1959), mass which descends from the stratosphere tends to maintain its original identity and is observed to exist in "sheets" of large horizontal and small vertical extent. As a result of this characteristic, these atmospheric layers have been called "stable laminae". Because these layers are observed to maintain their identity in space and time, it is reasoned that it should be possible to identify their quasi-conservative air mass properties such as specific humidity, potential vorticity, and potential temperature.

Conservation of specific humidity implies that if an air parcel contains a certain amount of water vapor whose weight exists in a given ratio to the entire weight of the parcel, then this ratio will be preserved independent of any changes in pressure, density, and temperature. This is true as long as the parcel maintains its original identity and no condensation or mixing processes have taken place. In general, stratospheric air which has intruded into the lower atmosphere is identifiable on a sounding by extremely low values of relative humidity. However, the humidity element in a radiosonde instrument is usually incapable of recording relative humidities lower than about fifteen per cent. Below this value the radio signal emits a high-pitched vibrating sound and thus is said to be "motorboating". For a "motorboating" humidity measurement the reported relative humidity is actually the maximum possible value which could be observed under those measuring conditions. Because of this, large errors often result from specific humidities which are calculated from the measured relative humidities in such dry layers (Kleinschmidt, 1959; Danielsen and Reiter, 1960).

Potential vorticity P of an air parcel is known to be a conservative property for air motions which

are adiabatic and frictionless. It is defined on an isentropic surface by

$$P = Q \ \partial\theta/\partial p \qquad (1)$$

where Q is the absolute vorticity of the air parcel, θ is potential temperature, and p is pressure. Careful analysis of the field of potential vorticity has shown that in actuality, P is not strictly conserved along a trajectory path (Staley, 1957, 1960; Reed and Danielsen, 1959). It may at times change by a factor of two or more over a short time as a result of the influence of friction and diabatic heating. However, air of stratospheric origin generally possesses potential vorticities which are as much as an order of magnitude greater than tropospheric air. Because the air mass to be studied probably originated in the stratosphere, it should possess potential vorticities which are appreciably higher than the mean tropospheric value. Therefore, potential vorticity is especially valuable as an additional check on the accuracy of this trajectory analysis if the wind field is sufficiently well known.

It must be emphasized that conservation of specific humidity and potential vorticity along a trajectory is a necessary condition, but by no means a sufficient one for insuring the accuracy of the calculated trajectory.

IV. ANALYSIS OF STABLE LAMINAE

In accordance with Danielsen's (1959) observation that descent of mass from the stratosphere occurs in "stable laminae", an attempt is made to establish the existence of such stable stratifications in the free atmosphere prior to the observed radioactive fallout increase. This is accomplished by a careful analysis of the radiosonde data as plotted on thermodynamic diagrams. It becomes evident that a shallow stable layer exists over a large region of the southwestern United States prior to the observed fallout maximum (Table 1). This layer is exceedingly dry and possesses values of potential vorticity of about 10×10^{-9} cm sec deg g^{-1}. In the way of comparison a reasonable mean tropospheric value for the anticyclonic side of the jet stream is 2.5×10^{-9} cm sec deg g^{-1}. The stable layer thus might be of recent stratospheric origin and possibly carries the radioactive debris which ultimately causes the observed surface increase.

Because of the relatively low wind speeds in the stable layer itself, its movement may be followed for three observation times prior to the large fallout increase (Fig. 5). On 29 March 1200 GMT the stable layer is observed over the California, Nevada, Utah region with a mean potential temperature of about 300K. 12 hours later it has moved slightly eastward and possesses an approximate mean potential temperature of 303K. At first a diabatic temperature increase of this magnitude in 12 hours appears large, but almost every sounding which contained the stable layer at this observation time was characterized by an adiabatic layer below the dry inversion. Since this increase was observed during the daylight hours, one may assume that the temperature increase is attributable to an upward flux of heat from the surface through the adiabatic layer. Twelve hours after this (30 March 12 GMT) the layer has moved still farther eastward and is again at a potential temperature of approximately 304K. It is now located just slightly to the west of the area of large surface fallout observed on 30 March 1600 GMT.

At 1200 GMT, which conforms to 0500 Mountain Standard Time, the air just above the surface is characterized by a typical night time temperature inversion (Fig. 6). Due to the higher static stabilities of the inversion layer at the surface, vertical exchange of mass will be inhibited until the thermal stratification becomes dry adiabatic in response to solar heating. Under the prevailing conditions of clear skies and low surface wind speeds, the nocturnal temperature inversion usually breaks up a short time after sunrise. This breakup occurs on the average about 0700 MST (1400 GMT) under these geographical and seasonal conditions.

Thus it may be assumed that the nocturnal inversion as observed (Fig. 6) did break up shortly after sunrise, and consequently an adiabatic layer below the debris carrying inversion was created. In the adiabatic layer a vertical exchange of mass then took place which dissipated the inversion and resulted in a transport of radioactive debris to the surface.

Also it is quite possible that the same process occurred to some extent the previous day over a layer of greater vertical thickness. This is quite compatible with the surface fallout measurements which are collected at 1600 GMT and provide a single measurement for air collected over a twenty-four hour period. The large fallout was first observed in the 30 March 1600 GMT collection which was shortly after the probable breakup time of the nocturnal inversion. The hypothesis that the descent to the surface occurs as a result of vertical exchange through the adiabatic layer thus appears to be justified.

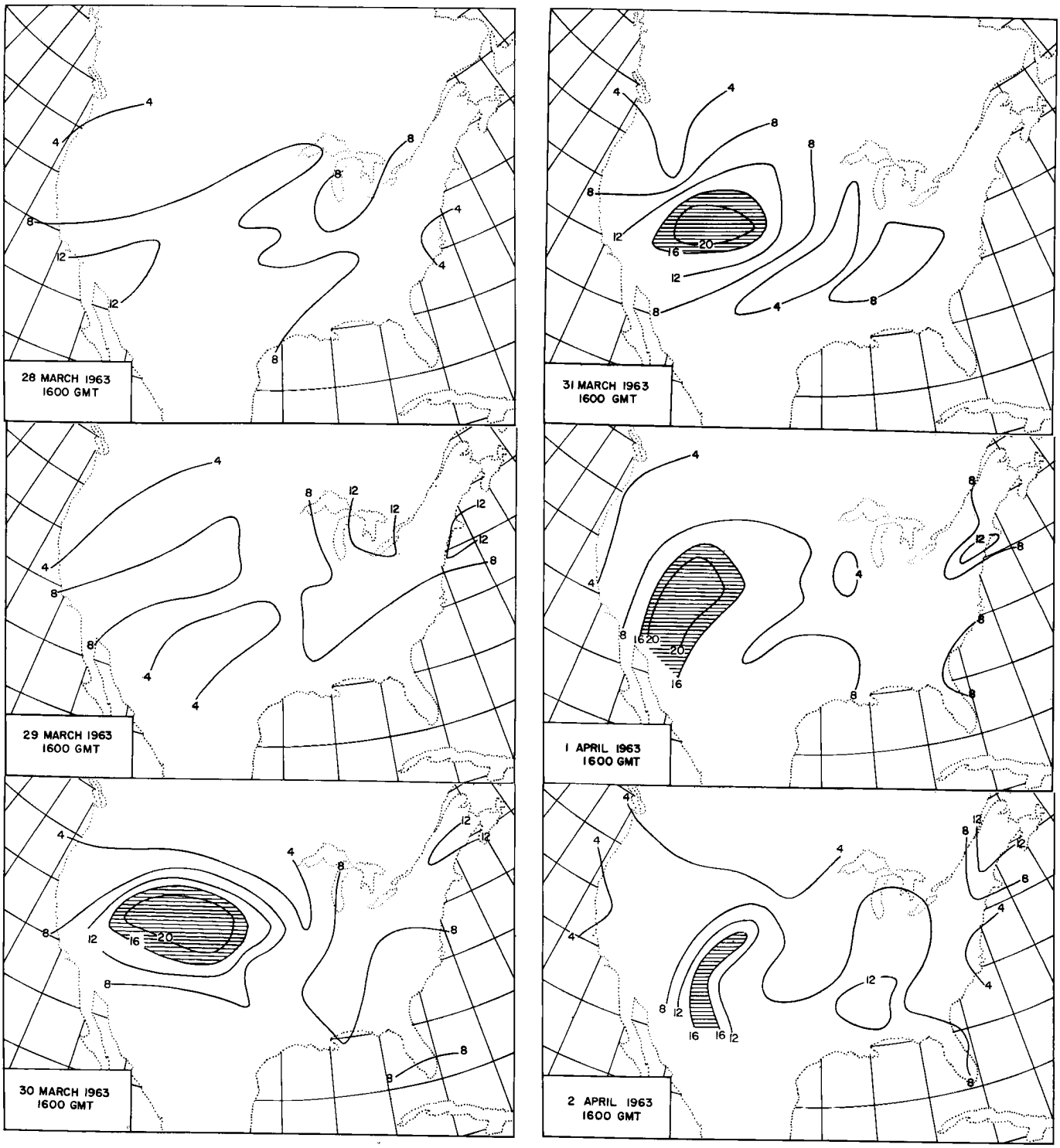

Figs. 4: Gross beta radioactivity in air for indicated dates in μμ curies per cubic meter. Areas with radioactivity greater than 16 μμ curies per cubic meter are hatched.

TABLE I

Tabulated values of mean relative humidity, mean wind speed in the stable layer and potential temperatures at the top and bottom of the stable layer for the indicated times. The prefix A in the relative humidity column denotes a "motorboating" report.

Station and Number		Boundaries of Stable Layer (Potential Temperature in Degrees K)	Relative Humidity	Mean Wind Speed (m/sec)
		29 March 1200 GMT		
San Diego	290	298-304K	A13	6
Santa Monica	295	299-304K	A13	10
Las Vegas	386	297-302K	A13	4
Grand Junction	476	297-300K	24	4
Ely	486	298-301K	18	9
Oakland	493	293-299K	A15	13
Salt Lake City	572	295-303K	A16	7
Winnemucca	583	297-303K	25	17
		30 March 0000 GMT		
Ely	486	303-308K	A17	20
Oakland	493	304-310K	A16	20
Lander	576	302-308K	A16	6
Winnemucca	583	297-304K	A20	20
San Diego	290	295-301K	A13	8
Santa Monica	295	298-304K	A14	9
		30 March 1200 GMT		
Santa Monica	295	304-307K	A14	9
Winslow	374	303-308K	20	9
Yucca Flat	385	301-308K	A14	8
Las Vegas	386	304-309K	A15	10
Denver	469	304-308K	A15	8
Grand Junction	476	304-311K	24	12
Ely	486	302-309K	A16	11
Salt Lake City	572	302-311K	A17	16
Lander	576	300-304K	25	23
		31 March 0000 GMT		
Las Vegas	386	301-306K	A14	8
Denver	469	311-314K	A16	14
Grand Junction	476	308-312K	25	15
Ely	486	304-309K	19	12
Salt Lake City	572	302-309K	A16	14
Lander	576	304-308K	25	15

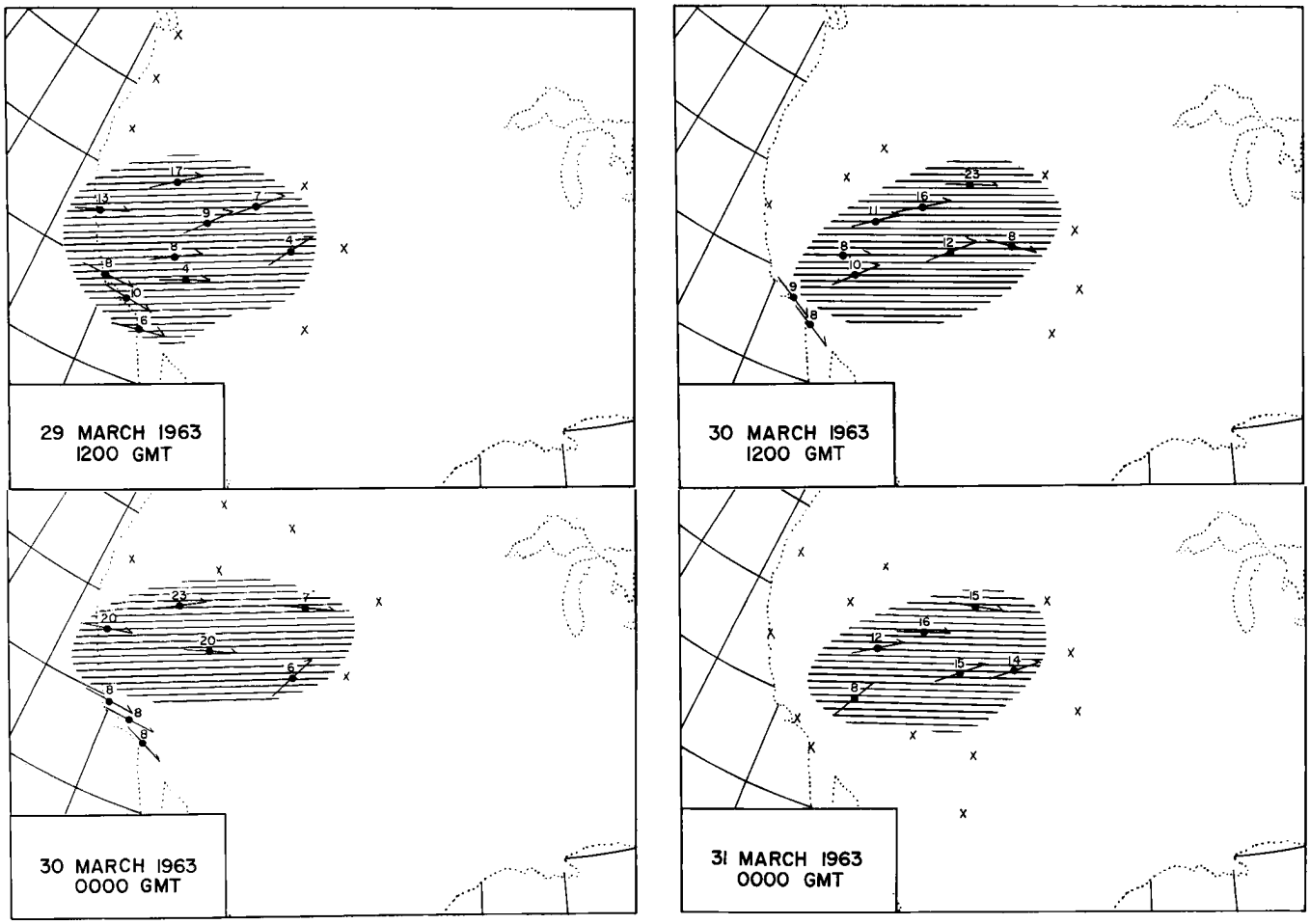

Figs. 5: Approximate spatial orientation of the dry stable layer for indicated dates. Mean wind speeds in the layer are given in meters per second. An x denotes a radiosonde station at which no stable layer was observed. Potential temperature thicknesses, relative humidities, and winds in the layer are given in Table I.

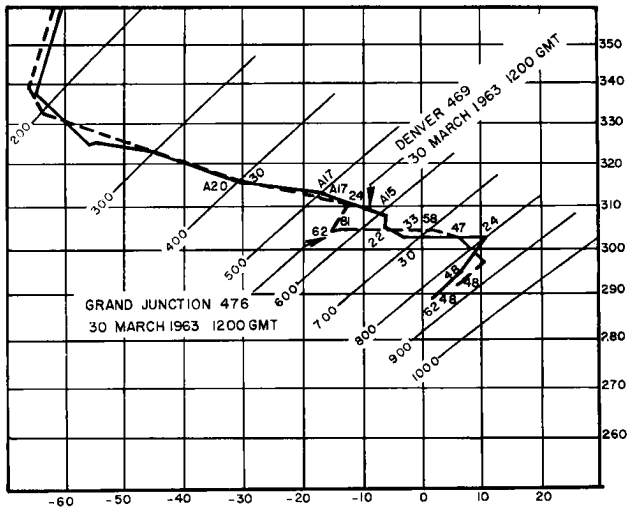

Fig. 6: Temperature soundings of Denver (469) and Grand Junction (476) for 30 March 1200 GMT plotted on a tephigram. Absicissa is temperature, ordinate is potential temperature, and the diagonal lines are pressure. Dark solid sounding and slanted numbers correspond to Denver (469). Dashed sounding and horizontal numbers are for Grand Junction (476). Plotted numbers are relative humidity values. Prefix A denotes a "motorboating" relative humidity report.

Heavy fallout was also observed on subsequent days and appears to move only slowly from its original position. The surface pressure systems were poorly defined in the area and the surface winds were very light. The high concentrations present on these days are then probably due to movement of the air in the surface layer and the final dissipation of the stable layer.

The amount of mass contained within this observed stable layer was crudely estimated over the time interval 29 March 1200 GMT to 31 March 0000 GMT, by integrating the mean pressure thickness of the stable layer over the area involved. The computed values are tabulated below.

29 March 63	1200 GMT	6×10^{11} metric tons
30 March 63	0000 GMT	4×10^{11} metric tons
30 March 63	1200 GMT	4×10^{11} metric tons
31 March 63	0000 GMT	2×10^{11} metric tons

The amount of mass contained in the stable layer appears to decrease as it moves eastward. This is probably due to a gradual depletion of the layer as a result of adiabatic mixing from below.

V. ISENTROPIC AIR TRAJECTORIES

There exist several different approaches to calculating air trajectories in the atmosphere. However, most of them are inapplicable for this type of study, because the assumption is made that the air particles move quasi-horizontally on a constant height or constant pressure surface. Because the trajectories are to be calculated for sinking air parcels, it is imperative that a procedure is employed which will take this into account.

Panofsky (1946) proposed that mean vertical velocities may be calculated by subtracting the initial height from the final height along an isentropic trajectory. In order for this technique to be useful, the stability of the air must be quite large so that the potential temperature surfaces are well defined at the level of interest. Also the condition that the parcel motion be dry adiabatic rules out the possibility of tracing ascending parcels of saturated air. Because the air masses which are to be investigated are descending and very stable. Panofsky's method appears to be quite applicable for this study.

Under present radiosonde coding procedures the calculation of isentropic trajectories is quite cumbersome, but the gain in accuracy and understanding of the vertical motion more than compensates for the increase in effort required. An adequately accurate air trajectory method has been derived by Danielsen (1961) and will be outlined here. If one considers the sum of the thermodynamic and mechanical energy equations for an air parcel of unit mass, one has for frictionless flow

$$dh/dt + \alpha\, \partial p/\partial t = d/dt(c_p\, T + gZ + V^2/2) \qquad (2)$$

where t = time
α = specific volume
T = temperature
V = wind speed
p = pressure
h = heat per unit mass
c_p = specific heat at constant p
g = acceleration of gravity
Z = height above mean sea level
$V^2/2$ = kinetic energy per unit mass

For adiabatic motions the potential temperature θ is conserved; thus with this assumption the trajectories will remain on a constant θ surface. θ is defined to be $T(1000/p)^{R/c_p}$ where R is the gas constant for dry air. If an isentropic stream function is defined as $M = c_p\, T + gZ$ one obtains for adiabatic flow

$$\alpha\, \partial p/\partial t = dM/dt + d/dt(V^2/2) \qquad (3)$$

The term $\alpha\, \partial p/\partial t$ may be expanded into isentropic coordinates by the transformation

$$\alpha\, \partial p/\partial t_z = \alpha\, \partial p/\partial t_\theta - \alpha\, \partial p/\partial Z\ \ \partial Z/\partial t_\theta \qquad (4)$$

Consider the derivative of $M = c_p\, T + gZ$,

$$\partial M/\partial t_\theta = c_p\, \partial T/\partial t_\theta + g\partial Z/\partial t_\theta \qquad \text{or}$$

$$c_p\, \partial T/\partial t_\theta = \partial M/\partial t_\theta - g\partial Z/\partial t_\theta \qquad (5)$$

By differentiating $\theta = T(1000/p)^{R/c_p}$ and assuming adiabatic conditions ($d\theta/dt = 0$), one arrives at

$$c_p \partial T/\partial t_\theta = \alpha\, \partial p/\partial t_\theta. \qquad (6)$$

Elimination of $c_p\ \partial T/\partial t_\theta$ from the previous two equations and substituting of the resultant expression for $\alpha\, \partial p/\partial t_\theta$ into the transformation equation yields

$$\alpha\, \partial p/\partial t_z = \partial M/\partial t_\theta - (g + \alpha\, \partial p/\partial Z)\partial Z/\partial t_\theta \qquad (7)$$

where the second term vanishes under the hydrostatic assumption.

By assuming that the total energy of a parcel

is conserved over a finite time interval the energy equation takes the approximate form

$$\int_{t_1}^{t_2} \partial M/\partial t_\theta \, dt = (M_2 - M_1)_\theta + \tfrac{1}{2}(V_2^2 - V_1^2)_\theta \qquad (8)$$

Here the subscripts 1 and 2 indicate the initial and final values along the trajectory path. This path is interpolated between two observation times (12 hours), and thus it is quite simple to find values for the initial and final points.

One may assume that the local change in stream function $(\int_{t_1}^{t_2} \partial M/\partial t \, dt)$ may be graphically determined by analyzing the 12 hour local changes of M at the data points and assigning a mean value for the trajectory interval. Also the approximate equation

$$D = \tfrac{1}{2}(V_2 + V_1)(t_2 - t_1) \qquad (9)$$

where D (distance traveled) must be satisfied for the trajectory interval.

Thus the objective is to locate a value of M at the final point such that both approximate equations are satisfied. This may be accomplished by a method of successive approximations for the final trajectory point and its accompanying value of M_2 on the given potential temperature surface.

In order that the values of M_1 and M_2 may be evaluated at the initial and final points of the trajectory, the fields of $M = c_p T + gZ$ must be calculated on the θ surface for the successive data times. A convenient way to calculate the height above mean sea level of the θ surface is to express it as the height of a nearby standard isobaric surface plus the thickness between the two surfaces. Hence,

$$M = c_p T_\theta + gZ_\theta = c_p T_\theta + gZ_p + g(Z_\theta - Z_p). \qquad (10)$$

By integration of the hydrostatic equation one obtains

$$Z_\theta - Z_p = -R\overline{T}/g \ln(p_\theta/p_p) \qquad (11)$$

where $\overline{T}$ denotes the mean temperature for the layer under consideration. Combining these

$$M = c_p T_\theta + gZ_p + R\overline{T} \ln(p_p/p_\theta). \qquad (12)$$

However, as pointed out by Danielsen (1959), quite large errors of M can be produced if the values of T_θ and p_θ are taken from the plotted soundings independently of each other. This difficulty may be circumvented by noting that T_θ and p_θ on an isentropic surface are related by Poisson's equation. By writing T_θ as a function of θ and p_θ, M can be written as

$$M = c_p \theta(p_\theta/1000)^{R/c_p} + gZ_p + 2.303R\overline{T}(\log_{10}p_p - \log_{10}p_\theta) \qquad (13)$$

(Reiter, 1963b). This form may be shown to yield values of M at any given θ level which are not more in error than heights computed for standard isobaric surfaces.

The question remains as to how accurate the trajectory calculations actually are. It is well known that any trajectory calculation is only an estimate of the actual air motion. An objective study by Djuric (1961) revealed that the largest errors in a trajectory analysis are due to the relative sparsity of radiosonde observations in many places and to inaccuracies in evaluating the actual wind speed. He finds that the factors of turbulent mixing and time interpolation are negligible compared to these. Thus even with the trajectory method outlined above, inaccuracies will have to be expected.

VI. CALCULATION OF THE AIR TRAJECTORIES

Since the air mass and mechanism which produced the observed fallout increase has been established to some degree of certainty, the ultimate source of this dry stable layer remains to be determined. This will be attempted by following the isentropic trajectory of this stable layer backwards in time by the method just outlined (for trajectory analysis and representative synoptic charts see Figs. 7 and 8. Because the upper air flow pattern does not vary appreciably over the time sequence of interest, only the isentropic analysis for 27 March 0000 GMT is included in the diagrams).

Since the final dissipation of the stable layer is accomplished by adiabatic mixing from below and not by actual contact of this layer with the ground, the analysis will be greatly simplified if the initial point of the trajectory is placed in the center of the well defined stable layer. As a result of this, the trajectory calculation was started at Las Vegas (386) on 29 March 1200 GMT on the θ = 300K surface. The θ = 300K surface intersected the center of the dry inversion at a pressure of 748 millibars (Fig. 9). This approach is advantageous, because the trajectory then begins at a data point so that quite accurate values of wind

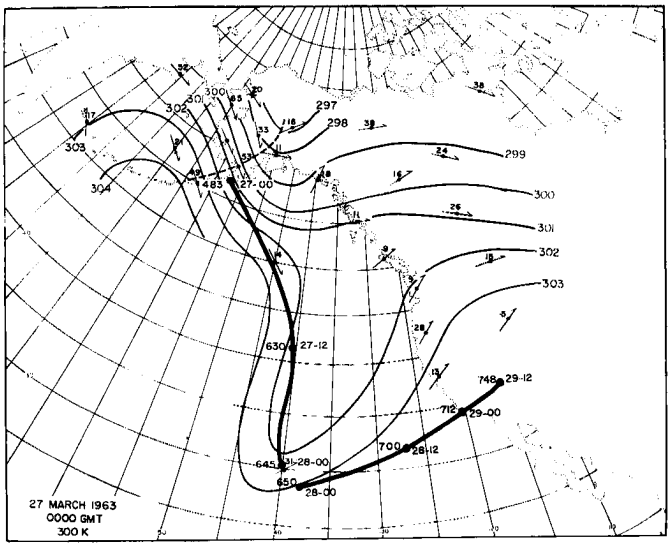

Fig. 7: 300K isentropic chart for 27 March 1963, 0000 GMT. Thin solid lines are isentropic stream function x 10^{-7} (ergs/gram). Arrows denote wind direction and plotted numbers above arrows are wind speed (m/sec). Heavy solid line represents the 300K isentropic trajectory traced backward from Las Vegas (386). Date, time, and pressure are plotted along the trajectory path.

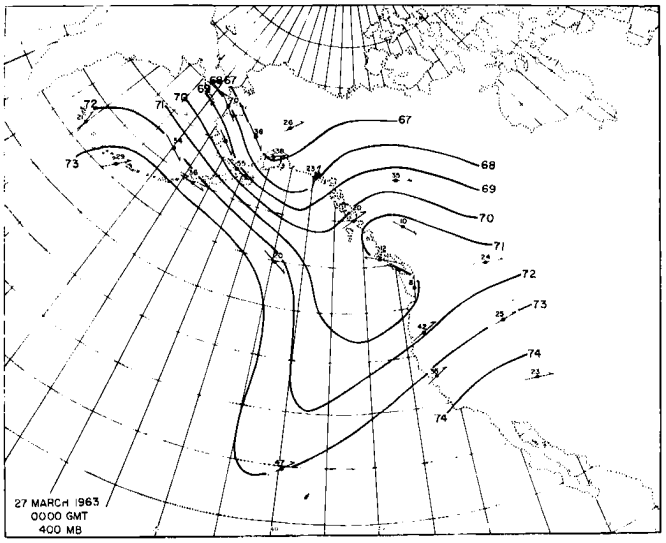

Fig. 8: 400 millibar isobaric chart for 27 March 1963, 0000 GMT. Pressure height values are given in hundreds of meters. Arrows denote wind direction and wind speeds are given in meters per second.

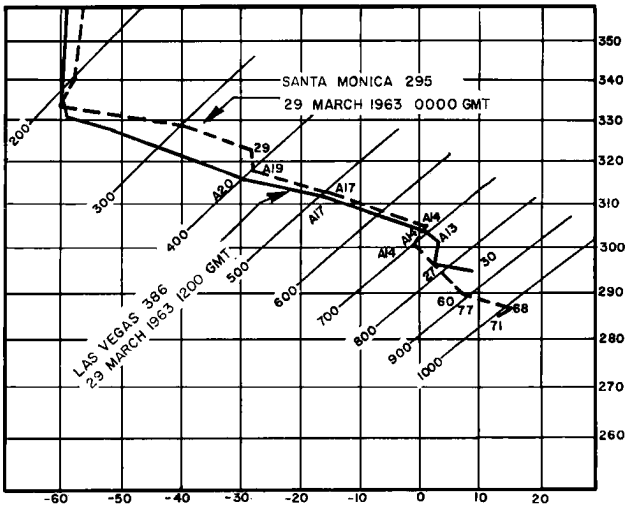

Fig. 9: Temperature soundings of Santa Monica (295) and Las Vegas (386) for indicated times plotted on a tephigram. Abscissa is temperature, ordinate is potential temperature, and the diagonal lines are pressure. Dashed sounding and horizontal numbers are for Santa Monica (295). Dark solid sounding and slanted numbers are for Las Vegas (386). Plotted numbers are relative humidity values. Prefix A denotes a "motorboating" relative humidity report.

speed and isentropic stream function are available.

Employing the trajectory method as outlined in the previous section, the parcel was traced backward over twelve hour intervals. At the end of the first interval the parcel was located just off the west coast of California near Santa Monica (295) (Fig. 7). The Santa Monica sounding for this date shows a very dry stable layer between the 300K and 305K potential temperature surfaces with the 300K surface located at 712 millibars (Fig. 9).

Twenty-four hours earlier the parcel was traced over the Pacific Ocean to a point about two degrees latitude from Weather Ship N. Investigation of this sounding reveals a dry stable inversion located between the potential temperature levels 299K and 315K (Fig. 10). The 300K level is now at a pressure of 650 millibars. The potential vorticity at θ = 300K for this sounding was approximately 19 x 10^{-9} cm sec deg g^{-1}, a very high value for tropospheric air on the anticyclonic side of the jet stream.

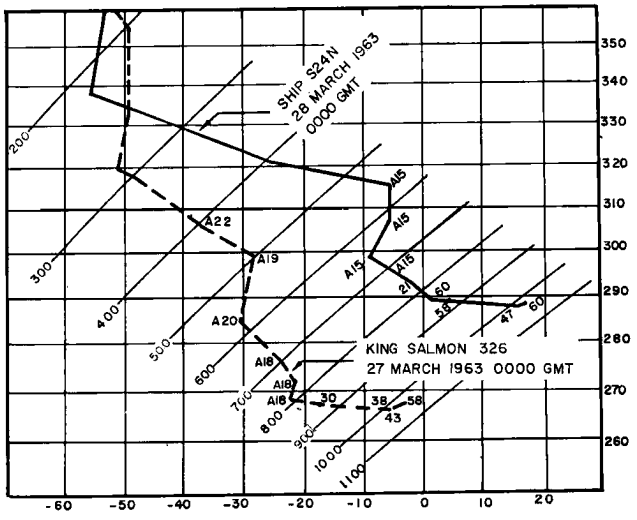

Fig. 10: Temperature soundings of Ship 24N and Alaskan station King Salmon (326) for indicated times plotted on a tephigram. Abscissa is temperature, ordinate is potential temperature, and the diagonal lines are pressure. Dark solid sounding and slanted numbers are for Ship 24N. Dashed sounding and horizontal numbers are for King Salmon (326). Plotted numbers are relative humidity values. Prefix A denotes a "motorboating" relative humidity report.

One could object, and quite legitimately so, that because of the lack of data over the Pacific Ocean, any type of trajectory calculation would be susceptible to serious errors. In order to minimize the uncertainty due to the scarcity of data, several precautionary measures were taken. To insure a more objective analysis of the stream function field, twelve hour local changes of M were recorded and analyzed over the entire isentropic chart. The stream function analysis was then made by taking the values of M from the previous analysis and the twelve hour local change into account. Also the stream function contour spacing was geostrophically checked against the available wind data. Conversely, when the air trajectory was located over an area with no wind data, a geostrophic wind was computed from the stream function field by the formula

$$V = -1/f \ (\Delta M/\Delta n)$$

where f is the Coriolis parameter and Δn is an increment of distance normal to the constant stream function lines.

Because the stable layer of interest is located over Ship N on 28 March 0000 GMT, and the computed parcel position was only a short distance away, the trajectory position was started anew at this point (Fig. 7). This procedure is advantageous, because it starts the trajectory from a data point; and it is located at a position in space where the stable layer is well defined. Again tracing the parcel backwards in time, it is seen to be experiencing quite strong decelerations along the trajectory path. The 28 March 0000 GMT and 27 March 1200 GMT wind speeds are twenty-one and thirty-seven meters per second respectively. It is also associated with rather pronounced cyclogenesis at this time and is located to rear of a high-level cyclone. In another twelve hour interval, the parcel position is very close to the Alaskan station King Salmon (326) (Fig. 7).

A check on the accuracy of the air trajectory to this point is obtained by calculating potential vorticity and specific humidity values for the trajectory points (Tables 2 and 3). Tables 2 and 3 reveal that potential vorticity and specific humidity apparently are <u>not</u> conserved along the trajectory path. Because the stable layer is a region of high potential vorticity values surrounded by air of lower values, it is reasonable to assume that potential vorticity would decrease along the trajectory path as a result of mixing and friction (Staley,

TABLE II

Approximate values of potential vorticity computed from soundings nearest to the trajectory points for indicated dates (Figs. 9 and 10). $P = Q\,\partial\theta/\partial p$ where the absolute vorticity $Q = f + V/R_s - \partial V/\partial n$.

Date	Static Stability $\partial\theta/\partial p$ deg cm $sec^2 g^{-1}$	Coriolis Parameter f sec^{-1}	Shearing Vorticity $-\partial V/\partial n$ sec^{-1}	Curvature Vorticity V/R_s sec^{-1}	Absolute Vorticity Q sec^{-1}	Potential Vorticity P cm sec deg g^{-1}
27 0000 GMT	2.0×10^{-4}	1.20×10^{-4}	$.27 \times 10^{-4}$	0.0	1.20×10^{-4}	29×10^{-9}
27 1200 GMT			Insufficient Data			
28 0000 GMT	2.8×10^{-4}	0.73×10^{-4}	-0.20×10^{-4}	0.13×10^{-4}	0.66×10^{-4}	19×10^{-9}
28 1200 GMT			Insufficient Data			
29 0000 GMT	2.3×10^{-4}	0.82×10^{-4}	-0.09×10^{-4}	0.02×10^{-4}	0.75×10^{-4}	17×10^{-9}
29 1200 GMT	1.3×10^{-4}	0.85×10^{-4}	0.0	0.0	0.85×10^{-4}	11×10^{-9}

TABLE III

Computed values of specific humidity for soundings nearest the trajectory position for indicated dates. The prefix A in the relative humidity column denotes a "motorboating" report. In a "motorboating" relative humidity report, the recorded values are the maximum possible under those atmospheric conditions. The calculated value of specific humidity is thus probably much higher than the actual value for a "motorboating" report.

Date	Relative Humidity r	Saturation Specific Humidity q_s	Specific Humidity q
27 0000 GMT	A19	0.7	0.13
27 1200 GMT		Insufficient Data	
28 0000 GMT	A15	3.1	0.46
28 1200 GMT		Insufficient Data	
29 0000 GMT	A14	5.0	0.70
29 1200 GMT	A13	6.3	0.82

1957, 1960; Reed and Danielsen 1959). The apparent increase of specific humidity along the trajectory path (Table 3) is justified in view of the uncertainties inherent in "motorboating" humidity reports. It is also reasonable that mixing processes would produce an increase in specific humidity along the trajectory.

VII. DESCENT OF STRATOSPHERIC AIR INTO THE TROPOSPHERE

Inspection of the King Salmon sounding for 27 March 0000 GMT shows a very stable stratification to exist in the layer from θ = 285K to θ = 300K (Fig. 10). The 300K surface is now located at a pressure of 485 millibars. Because the parcel is traced back to the Alaskan area, the increased data coverage makes it possible to analyze the spatial orientation of this stable layer. This is accomplished by constructing an atmospheric cross-section normal to the wind field from Cold Bay (316) to Fairbanks (261) (Figs. 11 and 12). Inspection of this diagram strikingly reveals that the stable layer suspect of carrying the observed radioactive debris is associated with the "jet-stream front" as described by Reed and Danielsen (1959), Staley (1960), and Reiter (1963a, b). Due to the high potential vorticity values present in this zone (see Table 2 for King Salmon value), it is thus inferred that this layer probably is the direct result of a strong sinking of stratospheric air into the troposphere.

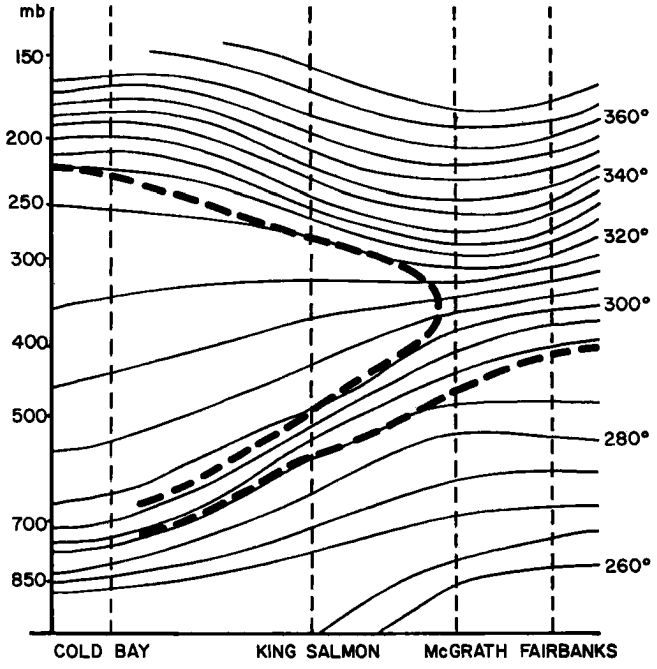

Fig. 11: Atmospheric cross-section of potential temperature and potential vorticity discontinuity for 27 March, 1963 0000 GMT. Cross-section is oriented normal to the 300K isentropic flow in the region of the computed trajectory position on this date. The flow direction is out of the plane of projection.

Because the 300K isentropic surface is only present on the cyclonic side of the jet core in the stratosphere, one has to conclude that the descent initially occurred on the cyclonic side (Fig. 11). However, an inspection of the cross section in Fig. 11 shows that the stable layer actually is oriented underneath and to the anticyclonic side of the jet axis. It is justly reasoned that an air parcel is physically unable to "cross" the jet axis because of the sharp gradients of potential vorticity and absolute vorticity at the jet core itself. However, Fig. 12 reveals that along the stable layer (as observed in the isentropic plane) no appreciable lateral shears are present; consequently, potential vorticity considerations present no barrier to this type of transport.

To obtain a further check on the reliability of this inference, potential vorticities were calculated and analyzed on the 300K isentropic surface over the area in which the sinking apparently took place (Fig. 13). On 26 March 1200 GMT all potential vorticities greater than 20 x 10^{-9} cm sec deg g^{-1} on the 300K surface are located in the stratosphere. Twelve hours later on the 300K surface, large values of potential vorticity (>20 x 10^{-9} cm sec deg g^{-1}) are also observed in the troposphere

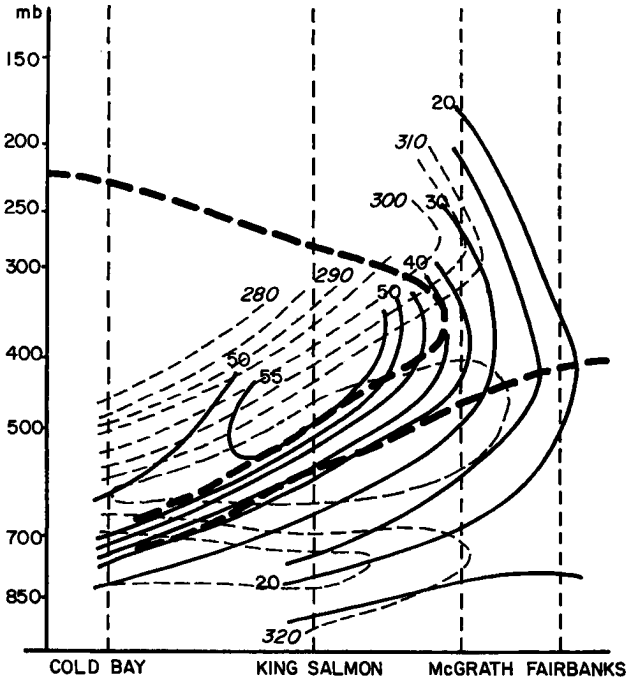

Fig. 12: Analysis of wind speed (m/sec and wind direction for same cross-section as in Fig. 11. The flow direction is out of the plane of protection.

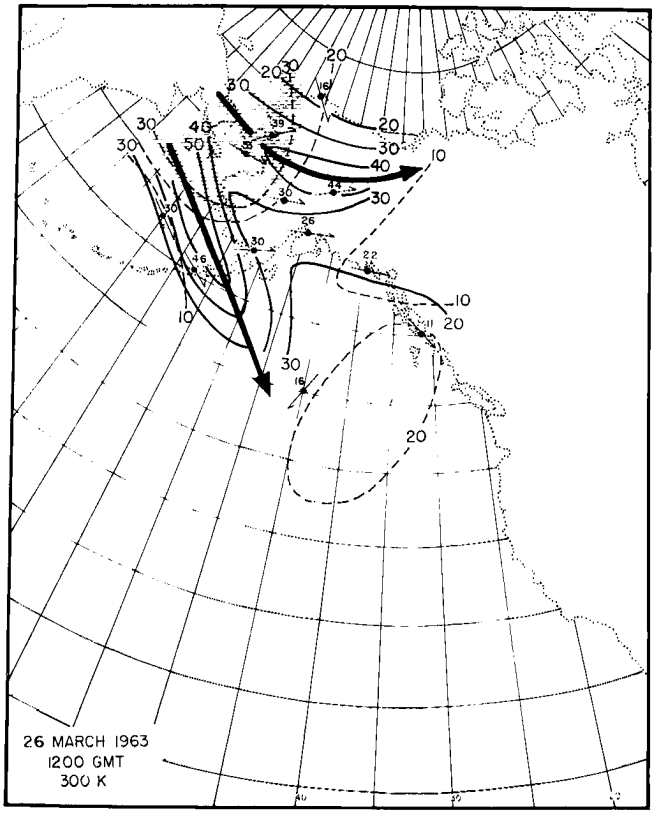

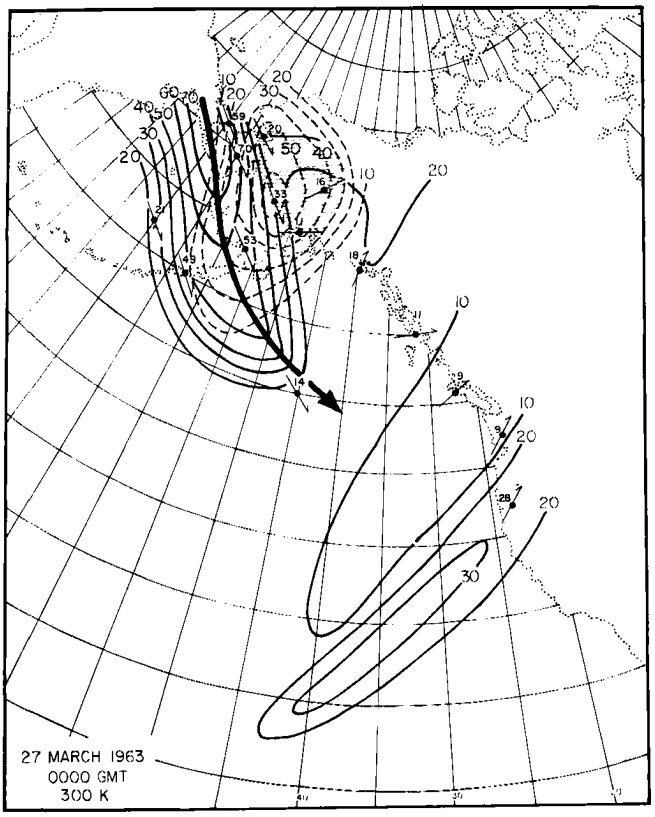

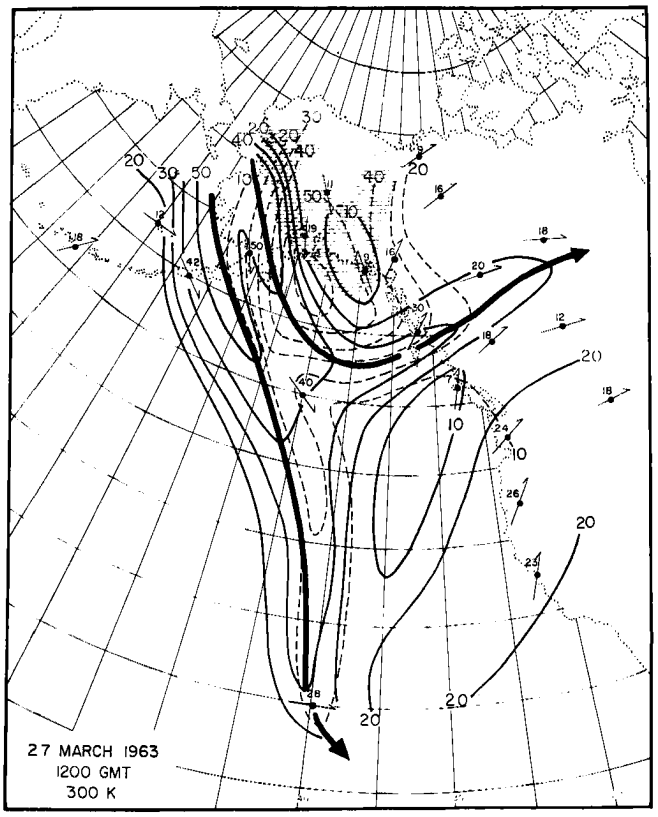

Figs. 13: Analysis of potential vorticity x 10^9 and wind speed on 300K isentropic surface from 26 March, 1963 1200 GMT to 27 March, 1200 GMT. Thin solid lines are isotachs (m/sec) and thin dashed lines are potential vorticity x 10^9 (cm sec deg/g). Light hatched region represents region where the 300K isentropic surface is in the stratosphere. Potential vorticities greater than 20 x 10^{-9} cm sec deg/g are associated with air of stratospheric origin.

(Fig. 13). The isentropic trajectories of this tropospheric high potential vorticity region trace backward to the stratospheric area in which the high values were initially observed. These large tropospheric values are thus a result of downward transport of air from this stratospheric high potential vorticity source. Since these high values are contained within the observed "jet stream front", one may infer that its appearance as a stable layer is due to the recent stratospheric origin of the air within it.

On 27 March 1200 GMT analyses of the wind and potential vorticity fields on the 300K isentropic surface reveal that this originally stratospheric stable layer splits into two distinct regions: one extending southward and following the rear of the trough; the other passing across the trough to the north (Fig. 13).

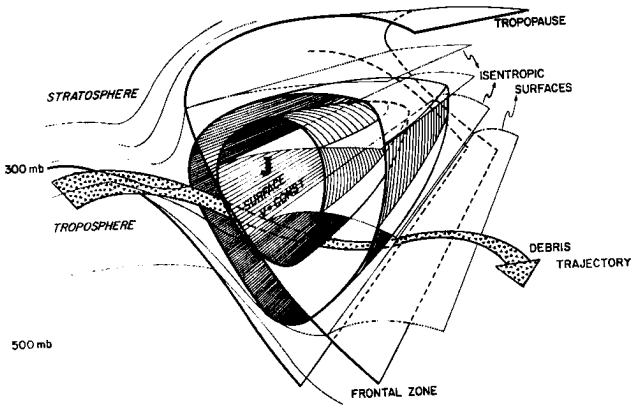

Fig. 14: Schematic trajectory of a radioactive debris-carrying air parcel (irregularly shaded arrows) in a three dimensional view of a relative coordinate system which moves with the jet maximum. Isentropic surfaces are indicated by thin lines; surfaces of constant wind speed, boundaries of the frontal zone, and the tropopause are marked by heavy lines. By the time the radioactive debris reaches the anticyclonic side of the jet stream after strong sinking, it will decelerate. It is still contained within a stable layer which now has the appearance of a subsidence inversion rather than of a strongly baroclinic frontal zone. In this diagram the flow direction is into the plane of projection (Reiter, 1963b).

It is now of interest to note the relative orientation of the winds on the 300K isentropic surface and the 400 millibar pressure level (Figs. 7, 8, and 12). The 400 millibar surface is chosen, because it represents the layer of maximum wind or jet stream level for this particular situation. At King Salmon the 400 millibar surface is approximately 1100 meters above the 300K isentropic surface. As noted before, the 300K isentropic surface is oriented along the dry stable layer that was followed in the trajectory study. Inspection of the wind directions in Fig. 12 shows that the 300K isentropic flow in the region of the cross section is actually "slipping under" the axis of strongest flow on the 400 millibar surface.

Thus, cold air which is originally on the cyclonic side of the jet stream can be subjected to a sinking motion which flows under the core of maximum wind and finally ends up on the anticyclonic side in a stable layer with relatively high potential vorticities (Fig. 14). It thus appears that the stable layer traced in the trajectory study is a result of this mechanism.

It has been hypothesized by several authors that descent of mass and radioactivity from the stratosphere to the troposphere is probably associated with high level cyclones (Storebø, 1959; Staley, 1960, 1962; Miyake et al., 1962). The findings of this study corroborate this hypothesis. It is further suggested that major descents of mass from the stratosphere are associated with cyclogenesis at jet stream level. However, more detailed studies will be necessary in order to establish the physical interaction between these two processes.

SUMMARY

An area of large increase of long-lived radioactive fallout is observed over a part of the western United States. In view of an estimated mean tropospheric residence time of one month, the air which carries this debris is inferred to have originated in the stratosphere.

By employing isentropic trajectories this debris-carrying layer is traced backward in time and eventually is seen to be a part of the "jet stream front". It is argued that this "front or baroclinic zone" consists of air which has descended from the stratosphere on the cyclonic side of the jet axis and "slipped under" this jet stream core. It is shown that this type of transport is consistent with the theorem of conservation of potential vorticity. This sinking is associated with a cyclogenetic

process which takes place to the rear of a high level cyclone.

ACKNOWLEDGMENTS

The author is especially grateful to Dr. Elmar R. Reiter for his patient guidance and counsel during the preparation of this report. He also wishes to give special thanks to Mr. Donald Beran and Mr. Gene Wooldridge for their technical assistance, and to Mrs. Viola Weiland who assisted in data preparation and typed the manuscript.

The data used for analysis was made available by the National Weather Records Center in Asheville, North Carolina, and by the U. S. Department of Health, Education, and Welfare, Public Health Service Radiation Surveillance Network.

REFERENCES

Bleichrodt, J. F., Joh. Blok, and R. H. Dekker, 1961: On the spring maximum of radioactive fallout from nuclear test explosions, Journal of Geophysical Research, 66, 135-141.

_____, Joh. Blok, and E. R. Van Abkoude, 1961: Origin of radioactive fallout in the northern hemisphere after the spring maximum in 1959, Journal of Geophysical Research, 66, 2183-2187.

_____ and E. R. Van Abkoude, 1963: On the deposition of cosmic ray produced beryllium-7, Journal of Geophysical Research, 68, 5283-5288.

Danielsen, E. F., 1959: The laminar structure of the atmosphere and its relation to the concept of a tropopause, Archiv für Meteorologie, Geophysik und Bioklimatologie, 11, 293-332.

_____, 1961: Trajectories: isobaric, isentropic and actual, Journal of Meteorology, 18, 479-486.

_____, and E. R. Reiter, 1960: Bemerkungen zu E. Kleinschmidt: Nicht-adiabatische Abkühlung im Bereich des Jet-Stream. Beiträge zur Physik der Atmosphäre, 32 (314) 265-271.

Djuric, D., 1961: On the accuracy of air trajectory computations, Journal of Meteorology, 18, 597-605.

Fry, L. M., F. A. Jew, and P. K. Kuroda, 1960: On the stratospheric fallout of strontium-90: the spring peak of 1959, Journal of Geophysical Research, 65, 2061-2066.

Greenfield, S. M., 1957: Rain scavenging of radioactive particulate matter from the atmosphere, Journal of Meteorology, 14, 115-125.

Gustafson, P. F., S. S. Brar, and M. A. Kerrigan, 1961: Appearance of a spring maximum in nuclear test debris in 1960, Science, 133, 460-461.

Kleinschmidt, E., 1959: Nicht-adiabatische Abkühlungen im Bereich des Jet-Stream. Beiträge zur Physik der Atmosphäre, 32($\frac{1}{2}$): 94-108.

Kruger, P., and C. L. Hosler, 1963: Sr-90 concentration in precipitation from convective showers, Journal of Applied Meteorology, 2, 379-389.

Libby, W. F., 1956: Radioactive strontium fallout, Proceedings of the National Academy of Science, 42, 365-390.

_____, 1959: Radioactive fallout particularly from the Russian October series, Science, 45, 151-175.

_____, 1961: Tritium geophysics, Journal of Geophysical Research, 66, 3767-3782.

_____, 1963: Moratorium fallout and stratospheric storage, Journal of Geophysical Research, 68, 2933-2937.

_____, and C. E. Palmer, 1960: Stratospheric mixing from radioactive fallout, Journal of Geophysical Research, 65, 3307-3317.

Lockhart, Jr., L. B., R. L. Patterson, Jr., A. W. Saunders, Jr., and R. W. Black, 1960: Fission product radioactivity in the air along the 80th meridian (west) during 1959, Journal of Geophysical Research, 65, 3987-3997.

Machta, L., and R. J. List, 1959: Analysis of stratospheric Sr-90 measurements, Journal of Geophysical Research, 64, 1267-1276.

_____, R. J. List, and K. Telegadas, 1962: A survey of radioactive fallout from nuclear tests, Journal of Geophysical Research, 67, 1389-1400.

Martell, E. A., 1959: Atmospheric aspects of strontium-90 fallout, Science, 129, 1197-1206.

_____, and P. J. Drevinsky, 1960: Atmospheric transport of artificial radioactivity, Science, 132, 1523-1531.

Miyake, Y., K. Saruhashi, Y. Katsurage, and T. Kanazawa, 1962: Seasonal variation of radioactive fallout, Journal of Geophysical Research, 67, 189-193.

Newton, C. W., and E. Palmen, 1963: Kinematic and thermal properties of a large-amplitude wave in the westerlies, Tellus, 15, 99-119.

Panofsky, H. A., 1946: Methods of computing vertical motion in the atmosphere, Journal of Meteorology, 3, 45-49.

Peirson, D. H., 1963: Beryllium-7 in air and rain, Journal of Geophysical Research, 68, 3831-3832.

Reed, R., 1950: The role of vertical motions in ozone-weather relationships, Journal of Meteorology, 8, 321-325.

_____, and A. L. Julius, 1951: A quantitative analysis of two proposed mechanisms for vertical ozone transport in the lower stratosphere, Journal of Meteorology, 8, 321-325.

_____, and E. F. Danielsen, 1959: Fronts in the vicinity of the tropopause, Archiv für Meteorologie, Geophysik und Bioklimatologie, 11, 1-17.

Reiter, E. R., 1961: The detailed structure of the wind field near the jet stream, Journal of Meteorology, 18, 9-30.

_____, 1963a: Jet Stream Meteorology, London, The University of Chicago Press, 515 pp.

_____, 1963b: A case study of radioactive fallout, Journal of Applied Meteorology, 2, 691-705.

Staley, D. O., 1957: A study of tropopause formation, Beiträge zur Physik der Atmosphare, 29, 1-22.

_____, 1958: Some comments on physical processes at and near the tropopause, Archiv für Meteorologie, Geophysik und Bioklimatologie, 10, 1-19.

_____, 1960: Evaluation of potential-vorticity changes near the tropopause and the related vertical motions, vertical advection of vorticity, and transfer of radioactive debris from stratosphere to troposphere, Journal of Meteorology, 17, 591-620.

_____, 1962: On the mechanism of mass and radioactivity transport from stratosphere to troposphere, Journal of the Atmospheric Sciences, 19, 450-467.

Storebø, P. B., 1959: Orographical and climatological influences on deposition of nuclear-bomb debris, Journal of Meteorology, 16, 600-608.

_____, 1960: The exchange of air between stratosphere and troposphere, Journal of Meteorology, 17, 547-553.

Tauber, H., 1961: Latitudinal effect in the transfer of radiocarbon from stratosphere to troposphere, Science, 133, 461-462.

Walton, A., and R. E. Fried, 1962: The deposition of beryllium-7 and phosphorus-32 in precipitation at north temperate latitudes, Journal of Geophysical Research, 67, 5335-5340.

HEAVY RADIOACTIVE FALLOUT OVER THE SOUTHERN UNITED STATES, NOVEMBER 1962

by

Elmar R. Reiter and J. D. Mahlman

ABSTRACT

Radioactive fallout in excess of 320 μμ curies per m^3 of air was observed over the south central United States on 24 to 27 November, 1962. Atmospheric transport processes leading to these abnormally high values of fallout were studied in detail. It was estimated that 6×10^{11} metric tons of air were involved in the rapid sinking process which transported air from the tropopause level to the ground in a matter of approximately two days. In spite of wet wash-out processes being in part involved in this case, the high-level origin of the contaminated air could be established from the analyses. The presence of a low-level jet stream and its associated precipitation system may have accelerated the wash-out process in this particular case.

I. INTRODUCTION

In previous studies (Staley, 1960, 1962; Reiter, 1963a, b, 1964; Mahlman, 1964; Danielsen, 1964) it has been shown that vertical transport processes near the jet stream constitute an effective mechanism for introducing stratospheric air into the troposphere. Reed's and Danielsen's (1959) "waterspout" model of the tropopause already contains the possibility of air masses moving isentropically within the "jet stream front" (Endlich and McLean, 1957) i.e., the stable layer found underneath the core of a jet stream.

High values of potential vorticity and of ozone (Danielsen, 1959; Murgatroyd, 1959; Reiter, 1961a, 1963c) as well as low humidities within this stable baroclinic region are of the same order of magnitude as those found in the lower stratosphere on the cyclonic side of the jet stream. From this we might conclude that the air contained within the jet stream front was not a product of mixing processes between the two adjoining air masses--as this might be the case for the low tropospheric portions of the polar-frontal zone--but constituted a third body of air imported from stratospheric levels.

After periods of nuclear testing--as was the case in November 1962--localized large concentrations of nuclear debris should be expected in the vicinity of the tropopause and in the lower stratosphere. Under the proper dynamic conditions contaminated air could then pass quickly through the "tropopause gap"[1] into the baroclinic "jet stream front" and hence into the middle and lower troposphere.

The previous cases under study (Reiter 1963a, b; Mahlman 1964) were concerned with radioactive fallout in dry air only. The case subsequently described was associated with wide-spread precipitation and thus contained the combined effects of both atmospheric transport and wet wash-out. With the data available only the atmospheric transport processes leading to the fallout could be considered.

In spite of these complexities induced by precipitation, the young age of the debris (some stations reporting 9 days) suggests a Soviet source. Table I lists the known events (U.S. Atomic Energy Commission, 1964).

---

[1]The "tropopause gap" is the discontinuity in tropopause level associated with jet streams.

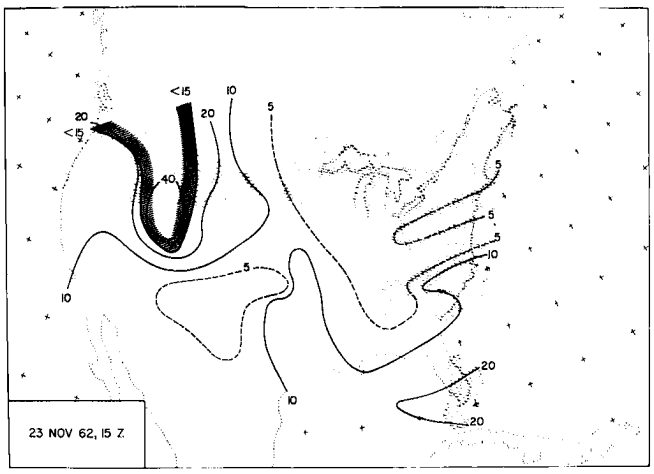

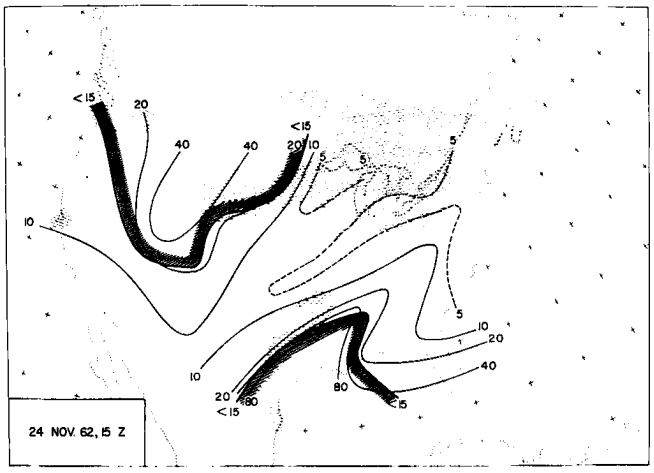

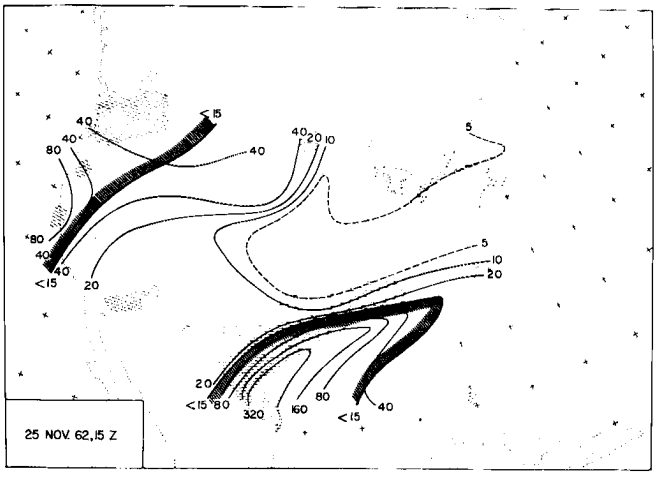

To Fig. 1

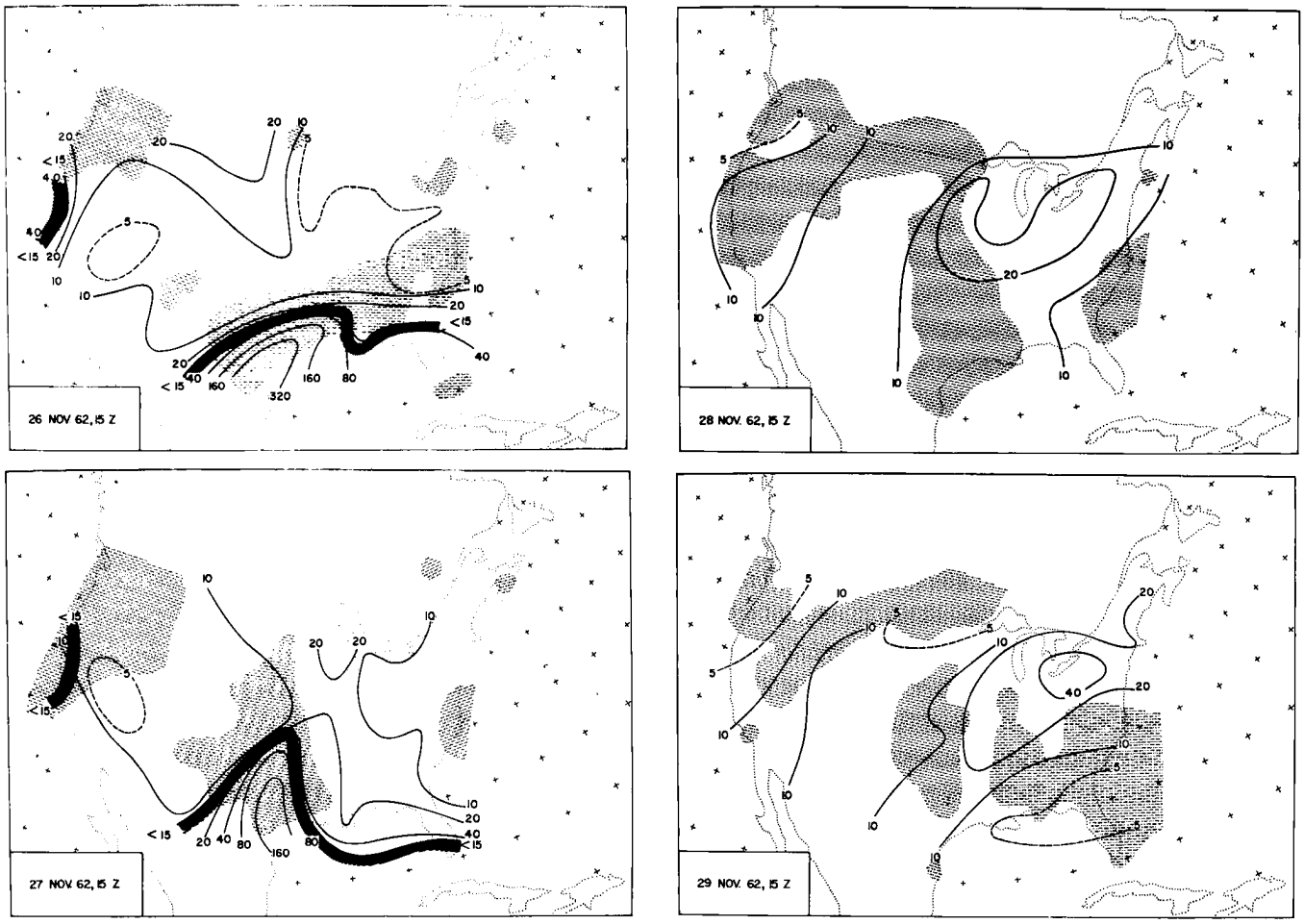

Fig. 1: Distribution of radioactive fallout from 23 to 29 November 1962 over the continental United States. Values are given in μμ curie per m^3 of dry air, as measured by the U.S. Public Health Service Radiation Surveillance network. Average collection time in the Central United States is 1500 GCT; filters are exposed for 24 hours. Lines labelled < 15 and marked by a shaded band enclose areas with debris age less than 15 days. Lightly shaded regions indicate precipitation during 24-hour period ending 0600 GCT as reported in the "Daily Weather Maps" of the U.S. Weather Bureau.

TABLE I: Atmospheric Nuclear Detonations

U. S. S. R., 1962

No.	Date 1962	Type	Yield	Location
27	1 Nov.	High Altitude	Intermediate	Central Asia
28	1 Nov.	Atmospheric	Intermediate	Novaya Zemlya
29	3 Nov.	Atmospheric	Intermediate	Novaya Zemlya
30	3 Nov.	Atmospheric	Intermediate	Novaya Zemlya
31	4 Nov.	Atmospheric	Intermediate	Semipalatinsk
32	17 Nov.	Atmospheric	Low	Semipalatinsk
33	18 Dec.	Atmospheric	Intermediate	Novaya Zemlya

The observed shift in fallout age over the southern United States to values less than 15 days and as low as 9 days (Fig. 1) suggests the event of 17 November over Semipalatinsk to be the primary source for the debris measured in dry air as well as in precipitation. This would give the debris approximately 4 days to travel to the North American west coast and three more days to appear at the ground over the southern United States. Such short time intervals would necessitate horizontal transport at or near the jet stream, even for the debris that was washed out by precipitation.

An estimate of trajectories from Semipalatinsk to the United States is being made in a separate investigation. In the following the transport processes over the United States leading to a rapid vertical movement of contaminated air through the troposphere are considered in detail.

II. ISENTROPIC TRANSPORT OVER THE UNITED STATES

An increase in fallout rate of relatively young debris (< 15 days) appears over the northwestern United States on 23 November (Fig. 1). The cause of this increase may rest with the same debris source that subsequently resulted in high fallout over south central United States. No closer investigation of the fallout on 23 November has been made, however, because the poor station coverage west of this fallout prohibited an accurate trajectory analysis.

On 24 November a distinct region of fallout in excess of 80 micro-micro curie/m^3 appears over the western gulf states. As may be seen from the precipitation area extending from Brownsville northward, part of this fallout was observed in dry air and part of it was associated with complex wet processes. It should be noted that from the previous day the debris age in this region shifted from approximately 30 days to less than 15 days (see Table II). This observed shift in mean debris age is an indication of the import of a different air mass which evidently traveled at jet stream speeds from its Soviet source region.

It is of interest to note that the precipitation band on 24 November over Texas and Oklahoma cuts across the strong gradient of fallout intensity. It also does on the subsequent days (Fig. 1). If washout processes were the primary cause of fallout, a close correlation should be expected between debris concentration pattern and precipitation pattern. Since this is not evident from the analyses, we may infer that in the present case the atmos-

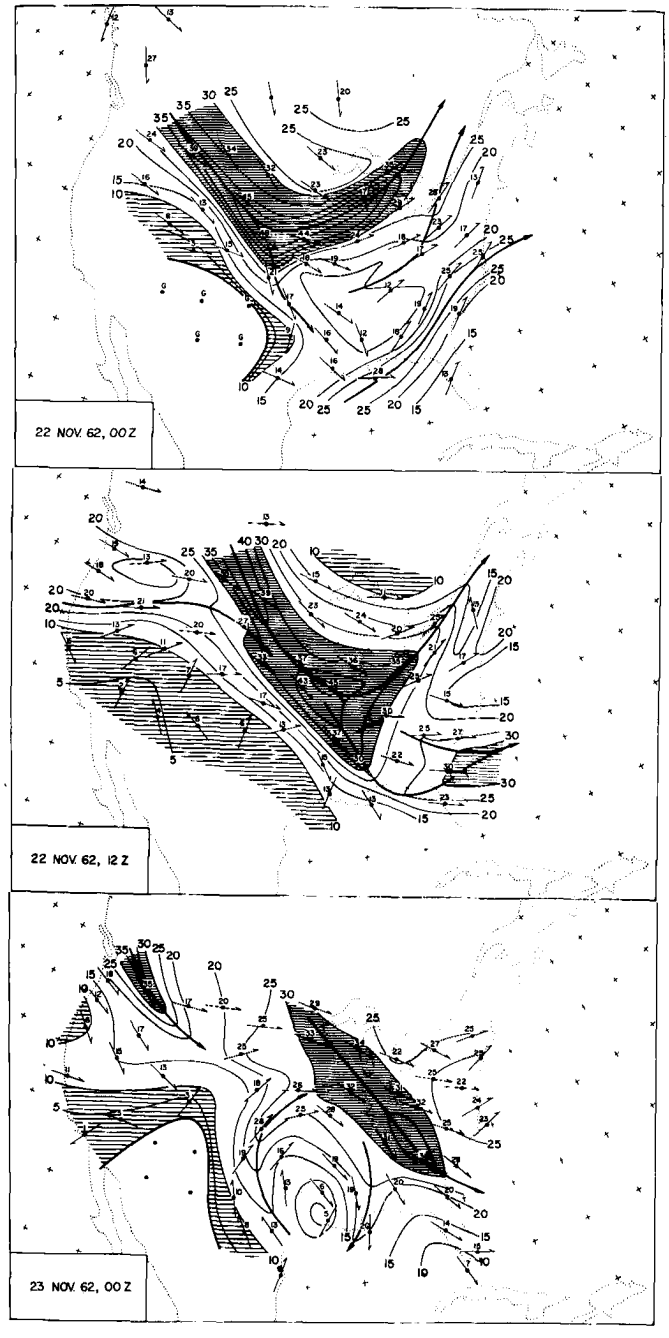

Fig. 2: Isotachs (mps) of isentropic surface 300K and for map times as indicated. Regions with speeds less than 10 mps and more than 30 mps are marked by different shading. Intersection of isentropic surface with ground is indicated by heavy line. Jet axes are shown by heavy lines with arrows. 300K surface not present at stations marked "G".

pheric transport processes of dry debris were of primary importance in generating the fallout area, and the observed precipitation only had a modifying influence on the deposition of radioactive nuclei.

Based upon this assumption, a detailed study of the transport processes of this case of radioactive fallout appeared feasible. The reliability of computed air trajectories is greatly enhanced if the air masses under consideration move isentropically. As may be seen from Table II, no precipitation was measured in Jackson, Mississippi, while high fallout concentrations were observed in dry air. Thus, at least for part of the fallout region, dry and quasi-adiabatic transport processes may be held responsible for the import of contaminated layers until these are tapped by the friction layer near the ground.

As has been stated in earlier papers, intrusions of air from jet-stream level into the lower troposphere are characterized by their relative dryness. Their humidity values usually are below the sensitivity threshold of the sensors carried by the radiosondes, thus giving rise to "motorboating" humidity reports.

Cross-sections through the fallout region (Fig. 13) reveal the existence of such a dry layer between 800 and 900 mb characterized by potential temperatures of 295 to 300K. Thus, for a detailed investigation of the dry transport processes during and preceding the fallout period, these two isentropic surfaces were chosen.

Fig. 2 shows isotachs (mps) of the 300K isentropic surfaces for 22 November 1962, 00 and 12 GCT, and 23 November 00 GCT. A distinct jet maximum may be seen advancing from the Northwestern into the Southeastern United States. Isobaric trajectory studies on the 300 and 400 mb surfaces over Asia and the Pacific Ocean led to the conclusion that this jet maximum could very well have contained debris from the low yield Russian event of 17 November.

These isotach analyses as well as others (Reiter, 1962) reveal strikingly that anticyclonic shear on isentropic surfaces tends to be stronger that cyclonic shear, a fact which normally is not realized along isobaric surfaces. Two criteria for limiting horizontal wind shears, derived by Arakawa (1951), for a zonal current are in agreement with this observation:

limiting anticyclonic shear

$$\partial u/\partial y = f + (U/R) \tan \phi \quad (\partial u/\partial y > 0) \qquad (1)$$

limiting cyclonic shear

$$-\partial u/\partial y = f/2 + (2U/R) \tan \phi \quad (-\partial u/\partial y > 0) \qquad (2)$$

(u is the zonal wind component; y is the poleward coordinate; earth's radius R=6.3712 x 10^6m; f is the coriolis parameter; ϕ is the latitude). For a mean speed u of 40 mps and a geographic latitude of 45° (Great Lakes region) one arrives at dynamic instability according to Eqn. (1) if anticyclonic shears exceed 12.19 mps per 60 nautical miles. This is equivalent to 10 mps per 0.82 deg. of latitude or 1.095 x 10^{-4} sec^{-1}.

On the cyclonic side of the jet stream instability should be expected with shears larger than 7.14 mps or 0.643 x 10^{-4} sec^{-1} given the same previous conditions.

Arakawa's criterion has been derived for the anticyclonic case by comparing the centrifugal force of an air parcel traveling under conservation of angular momentum with the centrifugal force of its environment. His criterion for the cyclonic case compares the excess centrifugal force of the displaced air parcel, constituting the turbulence generating force, with the Reynolds stresses representing the turbulence alleviating forces. Since both derivations involve motions of air parcels without external heat input, but under a perturbation of unspecified origin acting normal to the general direction of flow, the implicit assumption is that these parcels would be moving isentropically and that the Reynolds stresses should also be measured along isentropic surfaces. Consequently, lateral shears entered into Eqns. (1) and (2) should also be measured on isentropic surfaces rather than on isobaric surfaces.

Thus, Arakawa's instability criteria might be viewed with renewed interest, especially with regard to jet stream behavior. Isobaric shear characteristics would describe the jet stream properly only if quasi-horizontal motions along isobaric surfaces could be assumed (Kao and Hurley, 1962; Reiter, 1963d). This requirement quite obviously is not met in the vicinity of jet maxima.

Anticyclonic shears at 300K on 22 November 00 GCT 1962 to the southeast of the jet maximum are of the order of 15 mps/deg. latitude or 1.4 x 10^{-4} sec^{-1} (as compared with the limiting shear of 12.2 mps/deg. latitude according to Eqn. (1). Since streamline curvature in this region of strong horizontal shear is negligible, maybe even slightly negative values of absolute vorticity

$$Q = \frac{V}{R_s} - \partial V/\partial n + f \qquad (3)$$

TABLE II: Fallout measurements

(x indicates no precipitation sample for respective sampling period).

Station	Date	Radioactivity in Air $\mu\mu$ c/m^3	Mean Debris Age (days)	Precipitation over Sampling Period cm	Radioactivity in Precipitation $\mu\mu$ c/liter	Total Deposition $\mu\mu$ c/m^2
Miami, Fla.	23 Nov 13 GCT	25	16	X		
	24 Nov 13 GCT	69	16	X		
	25 Nov 14 GCT	30	22	X		
	26 Nov 15 GCT	51	12	X		
	27 Nov 13 GCT	50	13	X		
	28 Nov 13 GCT	6.6	27	X		
Jacksonville, Fla.	23 Nov 14 GCT	10	32	X		
	24 Nov 14 GCT	10	32	X		
	25 Nov 14 GCT	27	21	X		
	26 Nov 13 GCT	42	14	X		
	27 Nov 13 GCT	10	23	X		
	28 Nov 13 GCT	9.0	23	X		
Gastonia, N. Carolina	23 Nov 13 GCT	11	27	X		
	24 Nov 13 GCT	10	28	X		
	25 Nov 13 GCT	22	17	X		
	26 Nov 13 GCT	3.4	30	X		
	27 Nov 13 GCT	12	20	X		
	28 Nov 13 GCT	14	21	X		
Atlanta, Georgia	23 Nov 13 GCT	4.7	33	X		
	24 Nov 16 GCT	13	19	X		
	25 Nov	No Data or Sample Received				
	26 Nov 15 GCT	12	19			
	27 Nov	No Data or Sample Received				
	28 Nov 14 GCT	9.8	20	X		
Columbia, S. Carolina	23 Nov 15 GCT	7.4	32	3.20	570	18,000
	24 Nov	Motor Failure		X		
	25 Nov 17 GCT	25	14	X		
	26 Nov 15 GCT	3.6	29	X		
	27 Nov 15 GCT	7.7	22	X		
	28 Nov 15 GCT	10	22	X		
Jackson, Mississippi	23 Nov 15 GCT	7.0	26	X		
	24 Nov 15 GCT	78	9	X		
	25 Nov 15 GCT	203	10	X		
	26 Nov 15 GCT	108	11	X		
	27 Nov 15 GCT	27	19	X		
	28 Nov 15 GCT	14	22	X		

at selected stations

Station	Date	Radioactivity in Air μμ c/m^3	Mean Debris Age (days)	Precipitation over Sampling Period cm	Radioactivity in Precipitation μμ c/liter	Total Deposition μμ c/m^2
New Orleans, Louisiana	23 Nov 21 GCT	10	24	X		
	24 Nov 20 GCT	23	13	X		
	25 Nov 16 GCT	50	13	X		
	26 Nov 18 GCT	112	11	X		
	27 Nov 15 GCT	15	19	X		
	28 Nov 18 GCT	13	23	X		
Oklahoma City, Oklahoma	23 Nov 21 GCT	16	28	X		
	24 Nov 21 GCT	6.6	29	X		
	25 Nov	No Data or Sample Received				
	26 Nov	No Data or Sample Received				
	27 Nov 21 GCT	149	12	X		
	28 Nov 21 GCT	14	17	X		
Austin, Texas	23 Nov 15 GCT	12	24	X		
	24 Nov 15 GCT	102	9	0.62	4,300	27,000
	25 Nov 15 GCT	378	9	X		
	26 Nov 15 GCT	575	10	X		
	27 Nov 15 GCT	260	11	1.50	21,000	320,000
	28 Nov 15 GCT	11	16	X		
Little Rock, Arkansas	23 Nov 14 GCT	9.5	29	X		
	24 Nov 15 GCT	17	24	X		
	25 Nov 14 GCT	6.3	29	1.90	4,000	76,000
	26 Nov 14 GCT	12	24	X		
	27 Nov 14 GCT	22	24	1.48	5,900	88,000
	28 Nov	Filter Failure		0.11	7,200	8,100
Ponca City, Oklahoma	23 Nov 16 GCT	4.2	25	X		
	24 Nov 18 GCT	2.6	22	X		
	25 Nov 18 GCT	2.5	27	X		
	26 Nov 16 GCT	4.5	27	0.40	2,600	10,000
	27 Nov 16 GCT	37	12	1.98	6,600	130,000
	28 Nov 16 GCT	12	15	X		
Jefferson City, Missouri	23 Nov 14 GCT	8.5	31	X		
	24 Nov 14 GCT	5.9	31	X		
	25 Nov 14 GCT	3.3	27	X		
	26 Nov 14 GCT	5.8	28	X		
	27 Nov 14 GCT	29	17	X		
	28 Nov 14 GCT	25	21	X		

are to be expected here (V is wind speed; R_s is streamline radius; n is coordinate normal to flow direction. So far, isobaric analyses have only indicated the presence of regions with Q = 0 to the south of well developed jet maxima. Small values of negative absolute vorticity have been found from aircraft measurements (Reiter, 1961b, c, 1962), corresponding to a state of hydrodynamic instability (Arakawa 1941, 1942, 1951; Kleinschmidt, 1941a, b; Van Mieghem, 1944a, b).

The present analyses are based on radiosonde wind measurements known to be of good quality in the lower and middle troposphere. They suggest that dynamic instability may actually reach values significantly higher than the marginal values which result from isobaric analyses.

The discrepencies between isobaric and isentropic analyses may easily be explained with the aid of Fig. 3 showing a cross-section through the atmosphere from Green Bay (GRB), Wisconsin, to Oklahoma City (OKC), Oklahoma, on 22 November 12 GCT. This section cuts through the center portion of the advancing jet maximum. As has been pointed out earlier (Reiter, 1963a, b), isotachs and isentropic surfaces tend to run parallel inside the stable baroclinic zone underneath the jet core, often referred to as the "jet stream front". Thus, only small lateral shears should be expected along an isentropic surface within this zone. Isobaric lateral shears measured on more nearly horizontal surfaces will be appreciable in this same region. As may also be seen from Fig. 3, the isotachs bend up sharply in the troposphere after leaving the stable layer on the anticyclonic side of the jet stream. They intersect the isentropic lines more nearly perpendicular than the isobaric surfaces. This would render the isentropic shear in this region stronger than the isobaric one.

By similar reasoning, and as evident from Fig. 3, cyclonic isentropic shear should be less than cyclonic isobaric shear. There may also be a discrepancy between the locations of jet axes on an isentropic and an isobaric surface. Needless to say, for adiabatic motions, isentropic representations should be superior to isobaric charts in presenting the nature of jet streams.

The dispute on whether "horizontal" wind profiles should be "peaked" or "rounded" may also be resumed with the evidence presented here: Aircraft measurements mostly conducted with constant pressure altitude seem to indicate "peaked" profiles (Endlich and McLean 1957; Saucier, 1958 Reiter 1961a, 1963c). Isentropic profiles, according to Fig. 3, show hardly any lateral shear over some distance on either side of the jet axis. Thus, such profiles not only would be "blunt", but - in approximation - could be represented by a "plateau" of almost uniform strong winds with a drop-off in speed on either side.

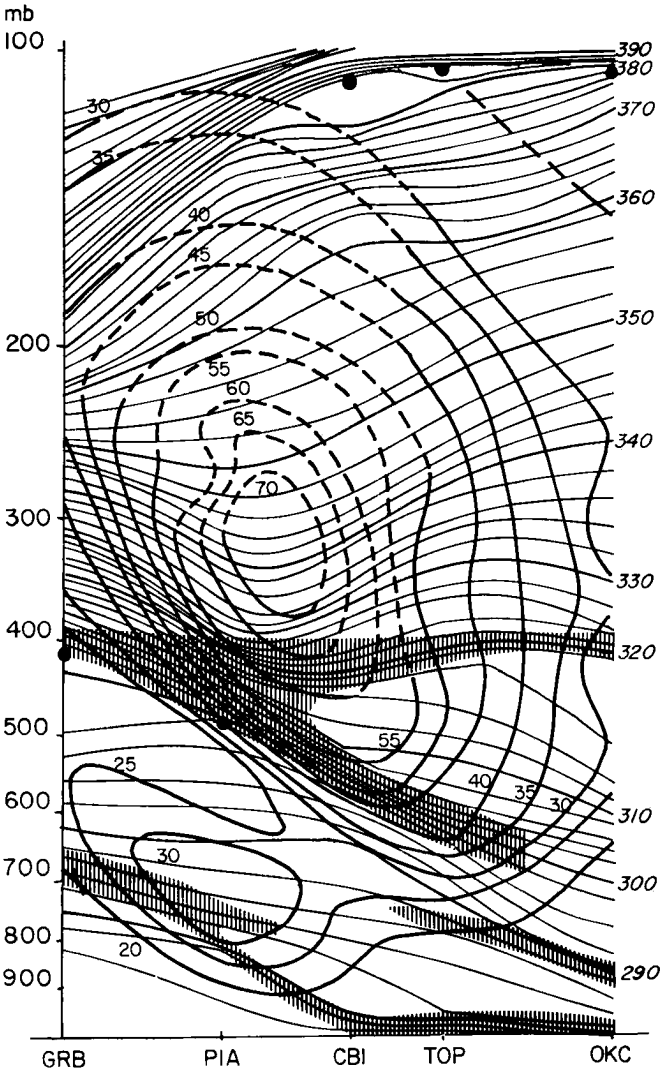

Fig. 3: Cross-section through the atmosphere from Green Bay (GRB), Wisconsin, to Oklahoma City (OKC), Oklahoma, 22 November 1962, 12 GCT. Heavy full and broken lines: Isotachs (mps, vertical numbers); thin lines: potential temperature (K), slanting numbers). Vertical hatching indicates stable layers. Heavy dots mark the coded tropopause levels.

In line with this reasoning, the sharpness of the peak in an isobaric wind profile could be taken as an indication of the abruptness with which a stable layer sloping along isentropic surfaces is encountered by the measuring aircraft.

In viewing Fig. 3 we find the 300K surface well embedded in the stable layer underneath the jet core, whereas the 295K surface characterizes the bottom of this layer over the stations Columbia (CBI) Missouri, and Topeka (TOP), Kansas. This explains why the jet stream is considerably better expressed along the 300K surface during the first part of the period under investigation than is the case along the 295K surface (Fig. 4).

Lateral shears in these analyses are not nearly as strong on 22 November 00 GCT as they are on 300K at the same observation time. By 23 November 00Z the flow pattern becomes rather well defined at 295K, possibly due to slight diabatic cooling effects in the sinking air masses. This would help to incorporate the 295K surface into the stable layer over a wider region than was the case 12 hours earlier.

Surface frontal systems have been entered in Fig. 4 to indicate weather developments. The jet stream which first appears on 22 November, and which is suspected of carrying the radioactive debris, follows in the wake of a cyclonic disturbance over the Great Lakes area (22 November 00 GCT). It signifies a cold outbreak with an anticyclonic regime following behind an advancing cold front (22 November 12 GCT to 23 November 00 GCT). A new frontal system appears on 23 November 00 GCT, and as it becomes stationary 24 hours later over the central United States, radioactive fallout begins to appear to the south of this front.

Again making reference to Fig. 1, we find that the precipitation band crossing the fallout gradient on 24 November 15 GCT also crosses the frontal system at 12 GCT of the same day. This rain band seems to line up with the axis of a weak wind maximum, indicated in Fig. 4 (24 November 12 GCT).

A low level jet stream, which is quite pronounced at 295K on 23 November, shall be commented on later.

As mentioned earlier, "motorboating" humidity values, especially when occurring in the lower troposphere, may be taken as indicators of air masses subsiding from higher levels (Kleinschmidt 1959; Danielsen and Reiter, 1960; Reiter, 1963a, b). Fig. 5 shows relative humidities along the 295K surface with dry ("motorboating" stations giving maximum possible humidities with prefixed letter "A") and moist (>80%) regions shaded differently.

From these analyses the advance of dry air in association with the jet stream of Fig. 4 may be seen clearly until 23 November 12 GCT. On subsequent charts the dry region which apparently contained the nuclear debris becomes incorporated in a surface anticyclone and decreases markedly in its horizontal extent.

Relatively high moisture values, possibly imported by the low level jet stream (23 November), are found immediately to the west of the dry (subsiding) air. The sharp moisture gradient between

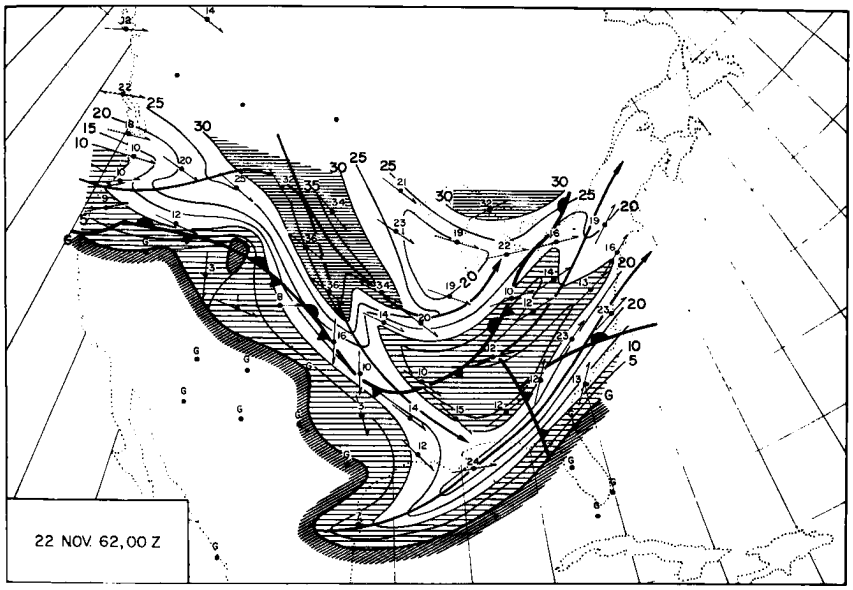

Fig. 4: Isotachs (mps) of isentropic surface 295K and for map times as indicated. Surface frontal systems have been entered. For further explanations see legend to Fig. 2.

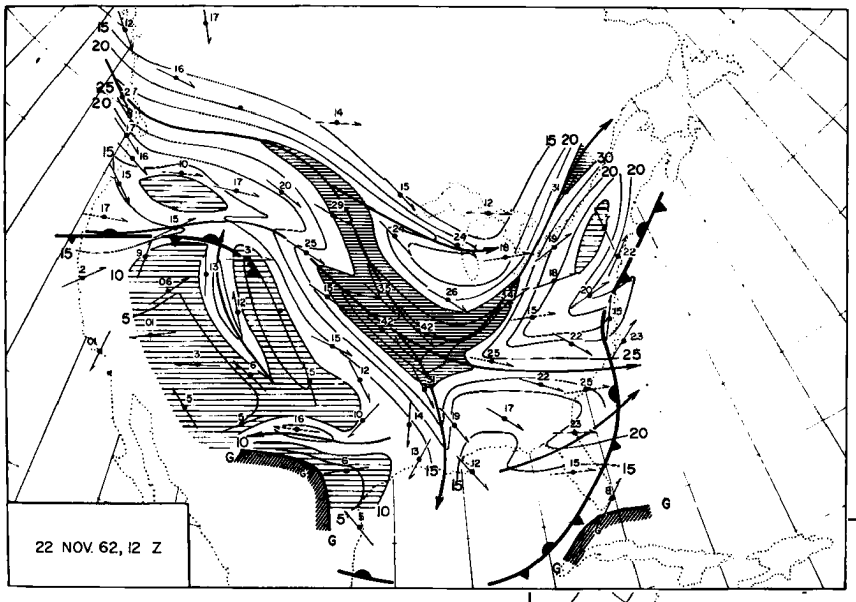

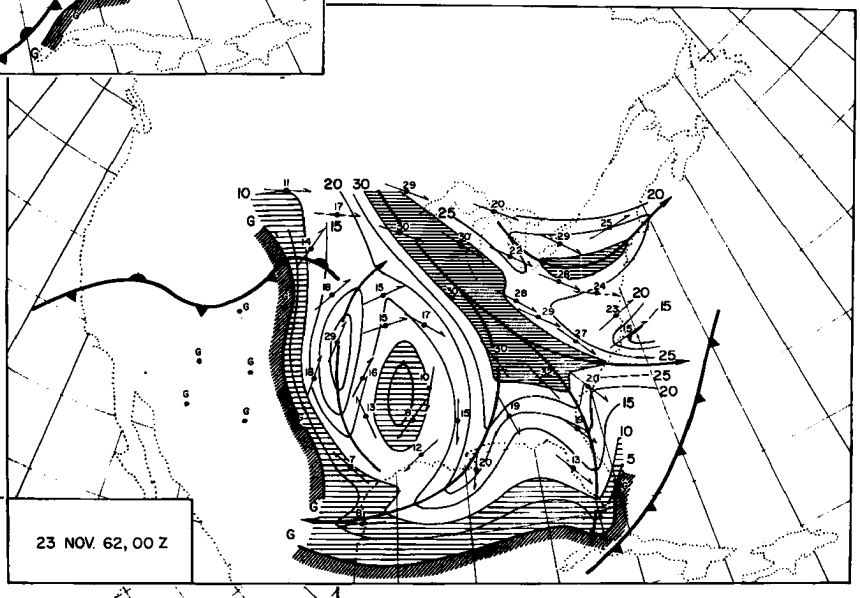

Fig. 4: continued

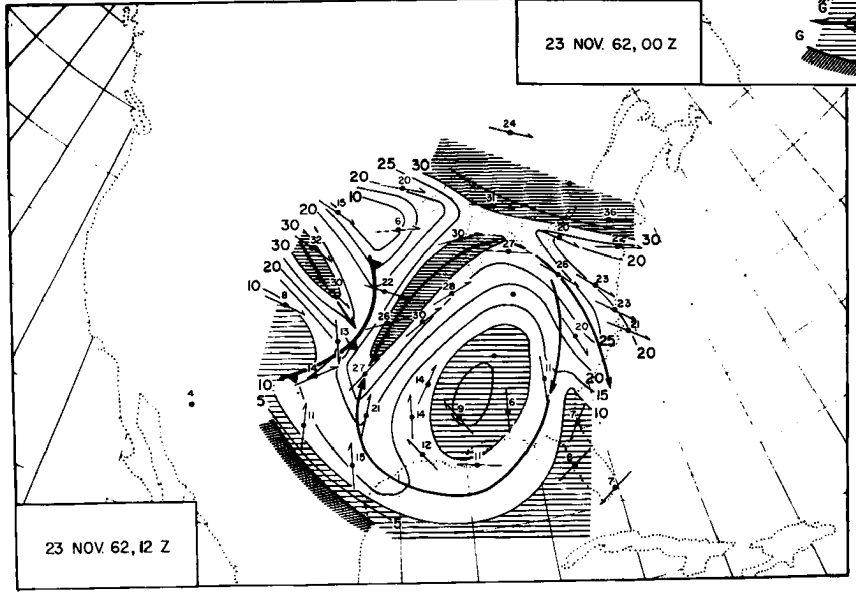

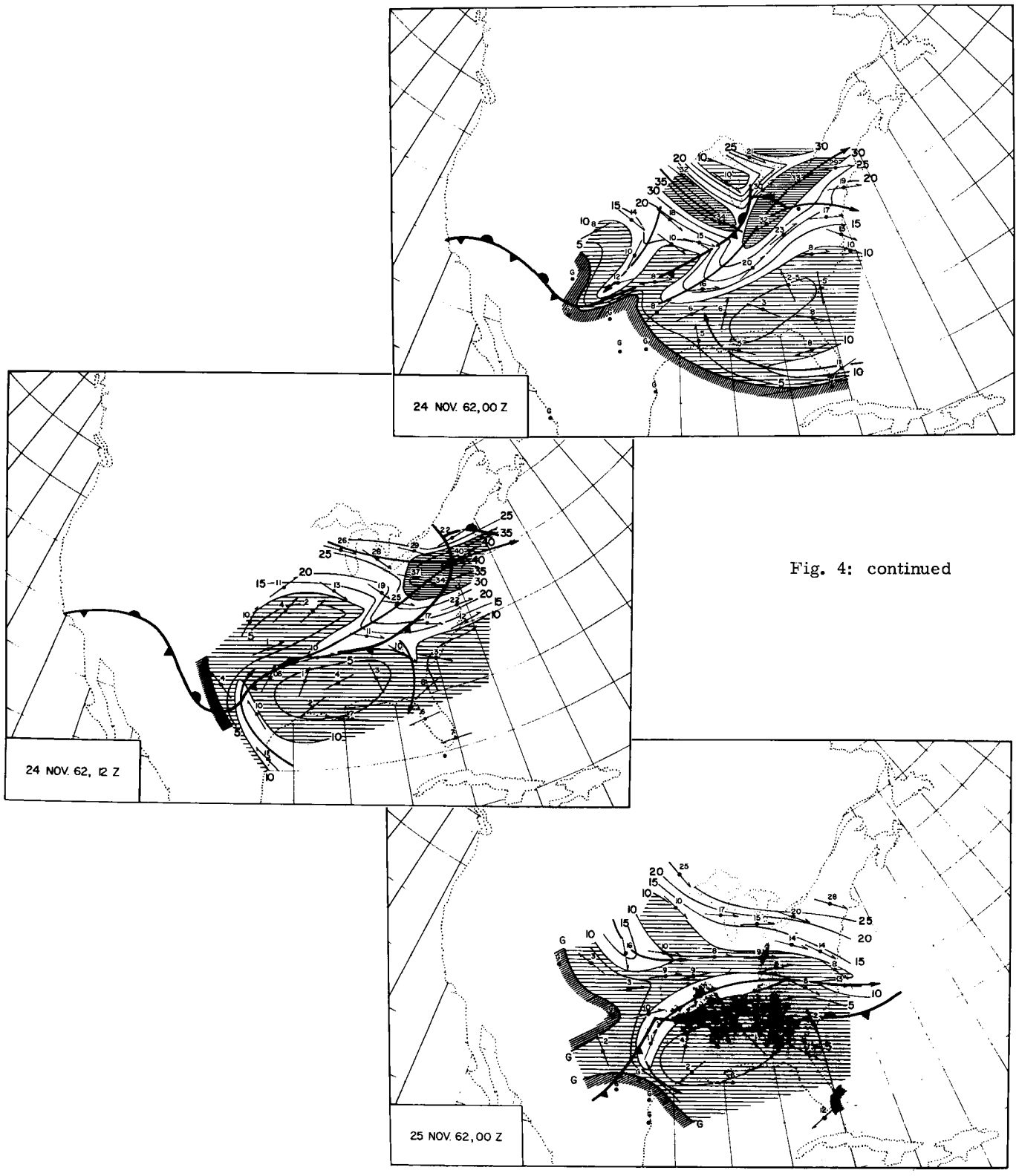

Fig. 4: continued

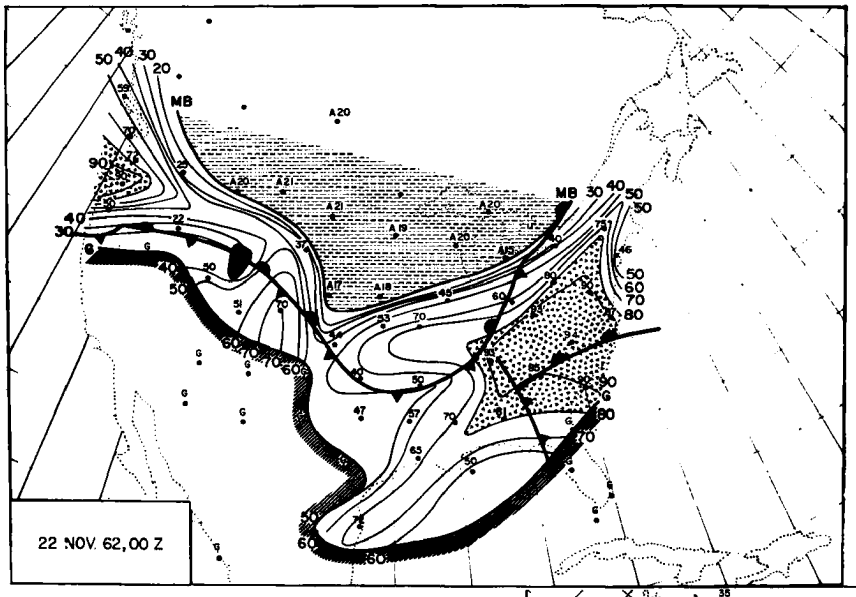

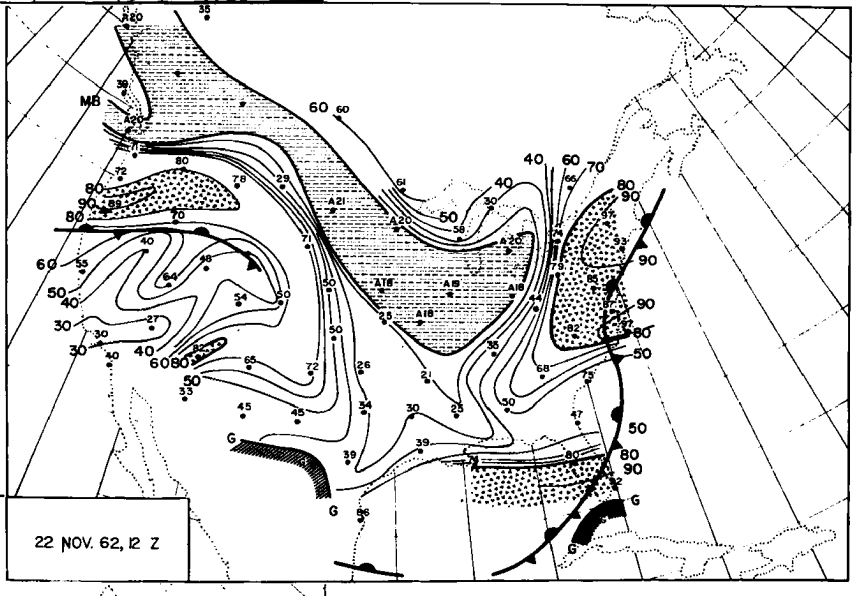

Fig. 5: Relative humidities (per cent) on isentropic surface 295K and for map times as indicated. Frontal systems as in Fig. 4. Areas with relative humidities in excess of 80 per cent and those with "motorboating" reports are marked by different shading.

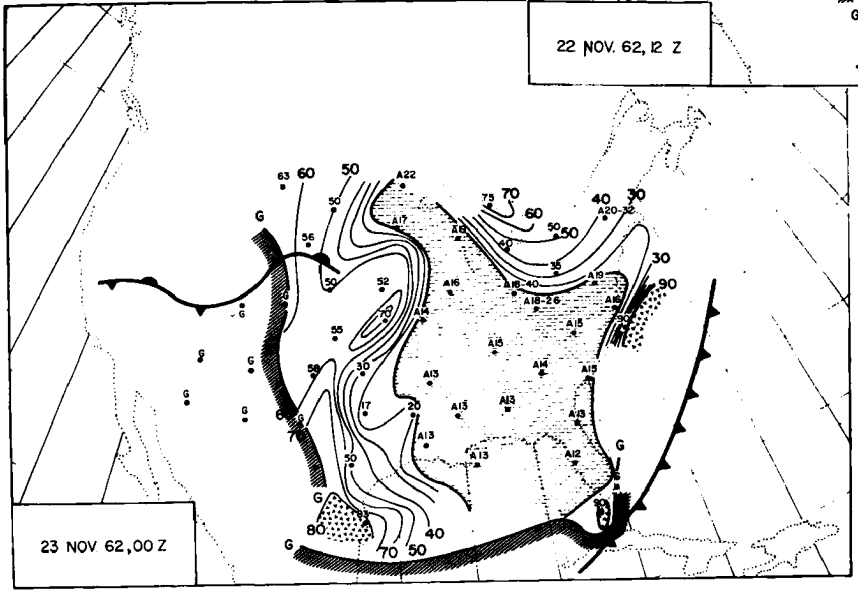

Stations in "motorboating" region are prefixed by letter "A" and give maximum possible humidity under such conditions. Intersection of 295K surface with ground is shown by heavy line, hatched band and "G".

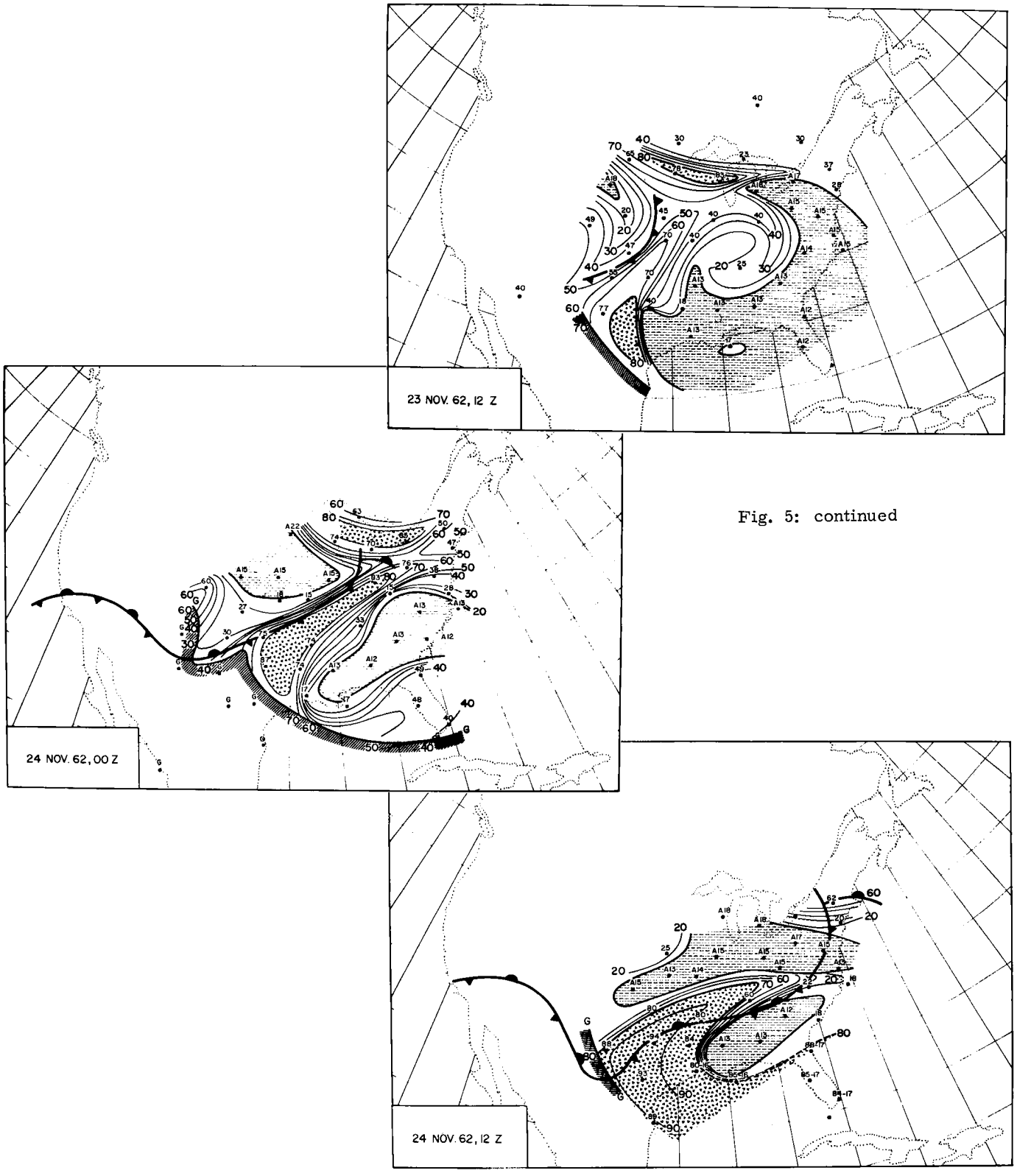

Fig. 5: continued

Fig. 5: continued

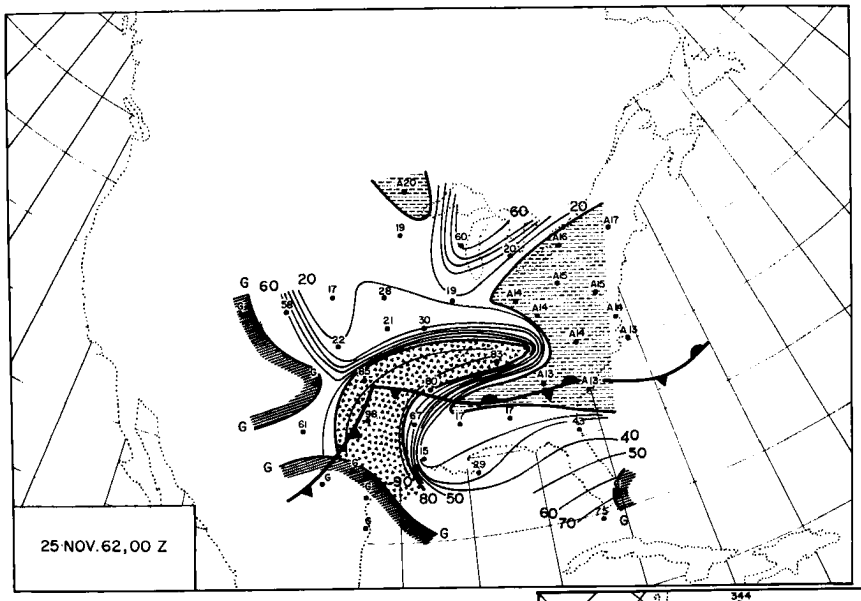

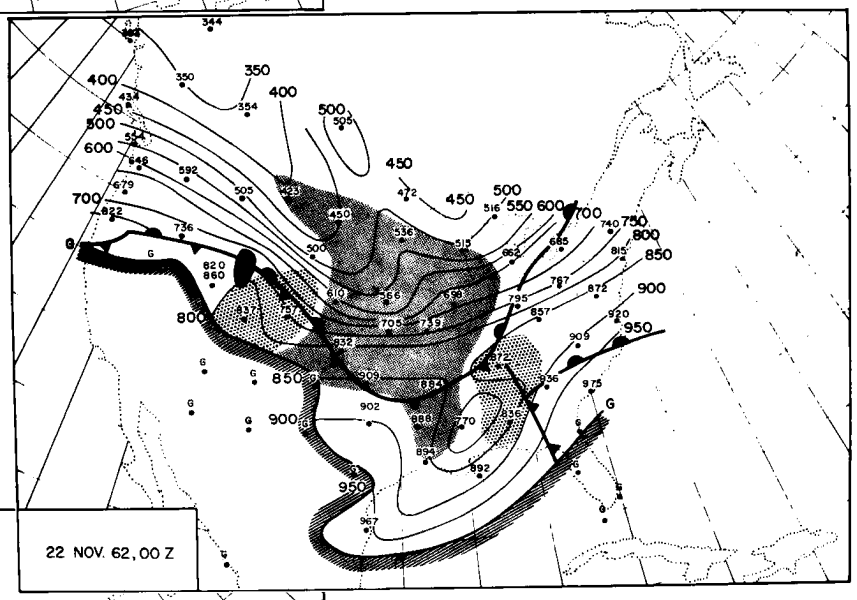

Fig. 6: Isobars (mb) of isentropic surface 295K and for map times as indicated. Frontal systems as in Fig. 4. Regions with $\partial p/\partial s > 0$ have been marked by narrow shading; regions with $\partial p/\partial s < 0$ by wide shading. Intersection of 295K surface with ground is marked as in previous figures.

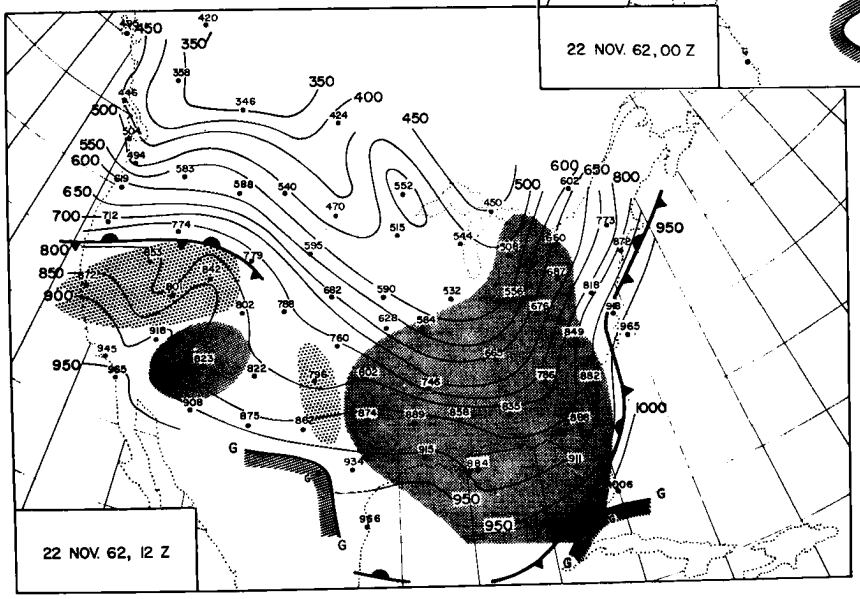

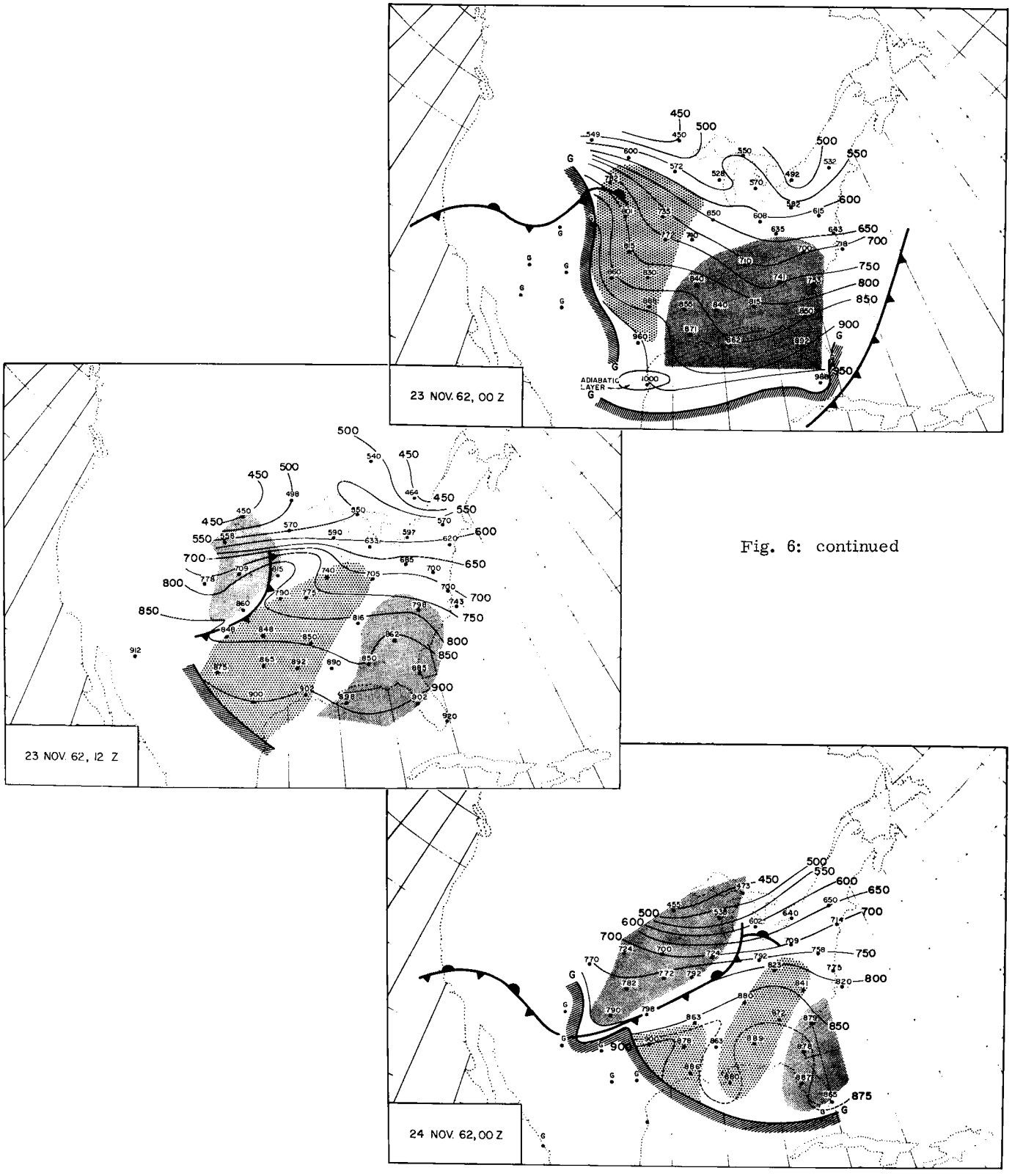

Fig. 6: continued

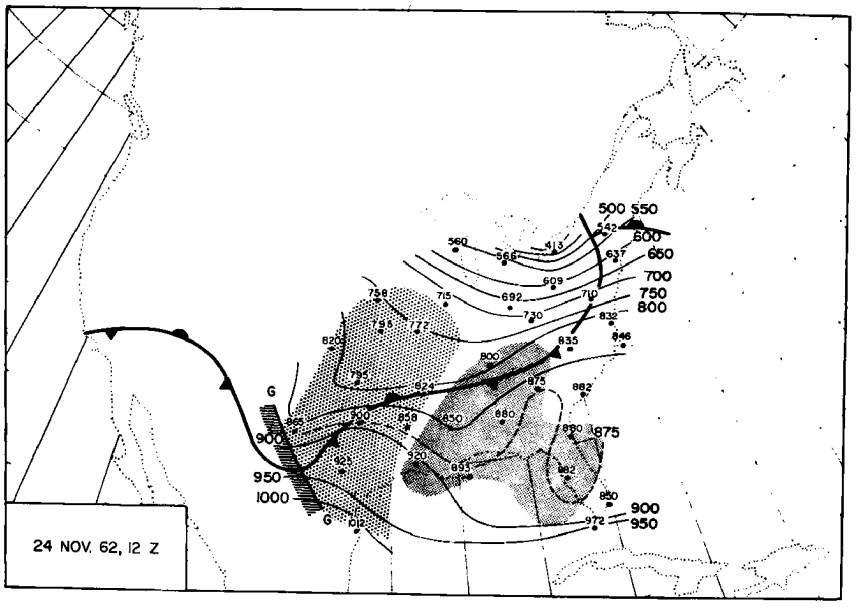

Fig. 6: continued

these two air masses on 23 November 12 GCT and 24 November 00 GCT outlines the boundaries between the entrance region of the low level jet stream (now preceding the new cold front) and the original cold outbreak (Fig. 5).

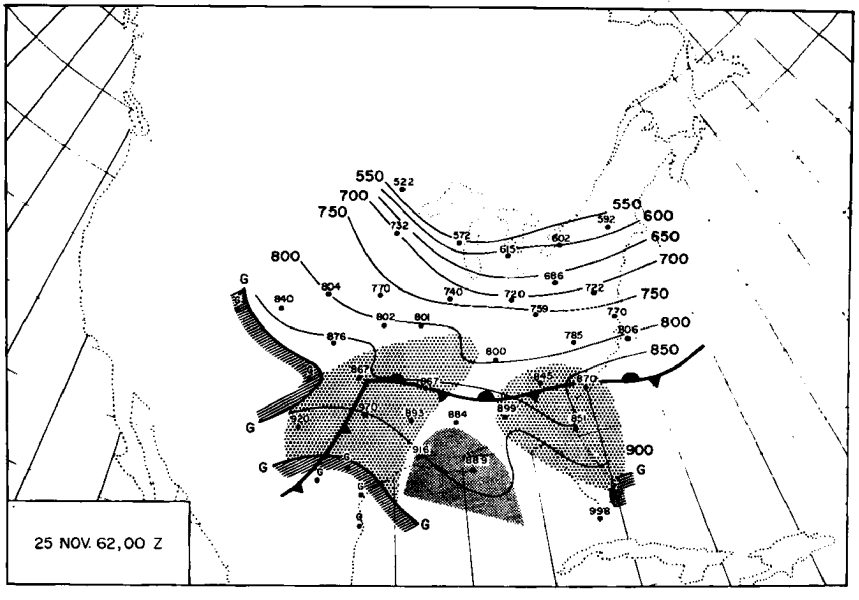

On 24 November 12 GCT and on the subsequent observation time a new surge of moisture advances from the Gulf of Mexico and overrides the quasi-stationary frontal system. This surge is carried by a very weak wind maximum (< 15 mps).

On 24 November moist air begins to occupy regions over Texas, Louisiana and Arkansas on the 295K surfaces, which on the previous day still contained "motorboating" reports. Since the trajectories that may be computed from the 295K surface do not indicate any retreat of the dry air, we have to conclude that the 295K surface no longer remains a substantial or physical surface for radioactive transport. This is evidently due to diabatic processes near the ground (downward mixing into the friction layer, as well as moist-adiabatic processes evident from the precipitation reports). The first appearance of high fallout values at the ground during the 24-hour sampling period ending 24 November 15 GCT is in excellent agreement with this conclusion (Fig. 1).

It is realized that relative humidity may serve only as a qualitative indicator of moist or dry air masses of different origin. Specific humidity would be a parameter more adequately considered con-

servative in the absence of precipitation processes, and thus more readily applicable to quantitative estimates. However, in view of the wide range of specific humidities that might be possible within the maximum values indicated for "motorboating" regions, such quantitative treatments would become meaningless in the analysis of dry subsiding air masses.

Fig. 6 shows pressure distributions along the 295K isentropic surface. On 22 November 00 GCT, when the debris-carrying jet maximum appears over the North Central United States, pressure values suggest a stratospheric origin of the air incorporated in this jet stream, especially when one considers the low tropopause values reported over Green Bay (GRB), Wisconsin, and Peoria (PIA), Illinois, shown in Fig. 3.

Qualitative indications of sinking and rising air motions (Fig. 6) (indicated by different shading for $\partial p/\partial s > 0$ and $\partial p/\partial s < 0$) are in excellent agreement with previous statements on wind systems and moisture distribution along this isentropic surface. For quantitative estimates of vertical motion, pressure variations along isentropic trajectories rather than streamlines will have to be considered.

III. QUANTITATIVE TRANSPORT COMPUTATIONS

In describing the short term or seasonal interchanges between stratosphere and troposphere it is of interest not only to establish the fact of such exchange processes, but also to arrive at magnitudes which may be viewed in the light of other evidence.

Estimates of the amount of air involved in the final deposition of debris near the ground will necessarily have to be based on assumed boundaries which limit the vertical and horizontal extent of this air mass. As one such condition, at least for horizontal extent, the dryness of subsiding air may be recognized. The limited accuracy of present humidity measurements, however, must be taken into account.

A further condition is available from the theorem of conservation of potential vorticity

$$\frac{dP}{dt} = \frac{d}{dt}\left(Q \cdot \partial\theta/\partial p\right) = 0 \qquad (4)$$

For stratospheric air originating from the cyclonic side of the jet stream and from a region of great thermal stability ($\partial\theta/\partial p$ large), high values of P should be expected.

Potential vorticity values in units of 10^{-9} x cm sec deg g^{-1} are given in Fig. 7 for the 300K surface, which at these observation times characterized the sinking stable layer. From an analysis of static stability and wind shear in the stratosphere, values of P=10 in the above units were somewhat arbitrarily chosen to outline the horizontal area of sinking air. This choice was substantiated by the fact that radiosonde data outside this boundary did not show a stable layer in the expected range of

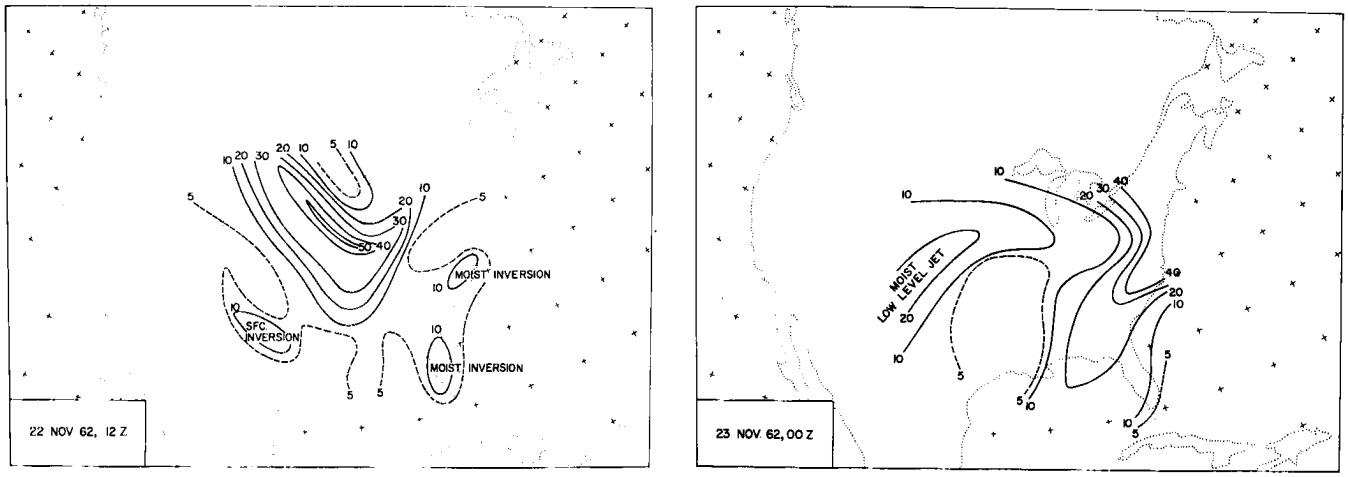

Fig. 7: Potential vorticity (units 10^{-9} cm sec deg g^{-1}) of 300K isentropic surface and for map times as indicated. Values greater than 10 (in above units) in dry air are indicative of originally stratospheric air.

potential temperatures. The strong anticyclonic wind shear observed along the boundaries of the stable layer was used as an auxiliary criterion in determining the extent of sinking air. This is in line with the discussion on wind shear in the previous section. The vertical dimensions of the sinking air were in first approximation considered to agree with the thickness of the stable layer containing the 300K isentropic surface, as evident from the radiosonde data.

In outlining the area of sinking air containing nuclear debris it became strikingly apparent that only the southern branch of the jet stream shown in Fig. 4 undergoes continuous and strong sinking motion. This splitting tendency of the jet stream is already indicated on 22 November 00 GCT (see also Fig. 2). Moreover, such a splitting tendency preceded the fallout events of September 1961 (Reiter 1963a, b) and March 1963 (Mahlman 1964).

At this point no explanation can be offered as to the causes of this splitting. Considering the strong anticyclonic shears observed at the time of splitting, we might conjecture that hydrodynamic instability exerts a certain influence. More research will be needed to arrive at an understanding of these processes.

Actual mass calculations performed in this case study considered only the branch of air which broke away from the jet stream in this splitting process, and which ultimately carried radioactive debris to the ground. Together with the other boundary considerations outlined above reasonable estimates were obtained in the following manner:

Values of Δp, i. e. the thickness of the stable layer in question, were analyzed within the outlined area (A). The integral $\int \Delta p/g \, dA$ was evaluated by planimetering sections of this area contained within isolines of Δp. The following results were thus obtained, using independent calculations for each observation time, without regard to time continuity in the analyses:

The last two values in this table involve a great deal of uncertainty because the area boundary advanced into the Gulf of Mexico and therefore could not be located accurately. The fact that all independent estimates stayed within the same order of magnitude should indicate that the region of sinking air could be bounded satisfactorily by applying the considerations outlined above. A certain amount of correction will have to be applied to these values, as will be shown in the following.

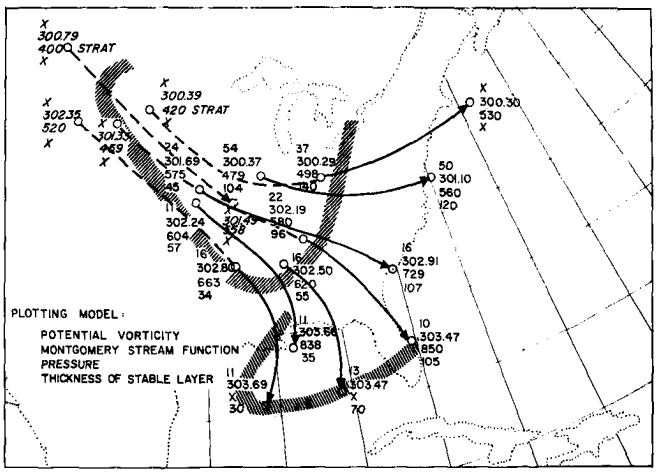

Fig. 8: Trajectories on 300K isentropic surface; from 22 November 1962, 00 GCT to 12 GCT: dashed lines; from 22 November 12 GCT to 23 November 00 GCT: full lines with arrows. Values of potential vorticity (units 10^{-9} cm sec deg g^{-1}), of Montgomery stream function (units 10^7 cm^2 sec^{-2}), of pressure (mb) of 300K surface, and of thickness (mb) of stable layer are entered numerically according to plotting model: slanting numbers for 22 November 00 GCT, vertical numbers for other map times. The centers of the hatched bands mark bounderies at 22 November 12 GCT and 23 November 00 GCT of contaminated air from tropopause level which reaches the ground over the southern United States.

TABLE III: Amount of air involved in radioactivity transport to the ground (uncorrected values)

Date	Calculated Mass Units 10^{12} Metric Tons
23 November 00 GCT	0.87
23 November 12 GCT	0.98
24 November 00 GCT	0.79
24 November 12 GCT	1.0

Fig. 8 contains 300K isentropic trajectories of air parcels located within the contaminated layer, described and computed above, whose outlines at 22 November 12 GCT and 23 November 00 GCT are indicated by hatching. (The center of the hatched

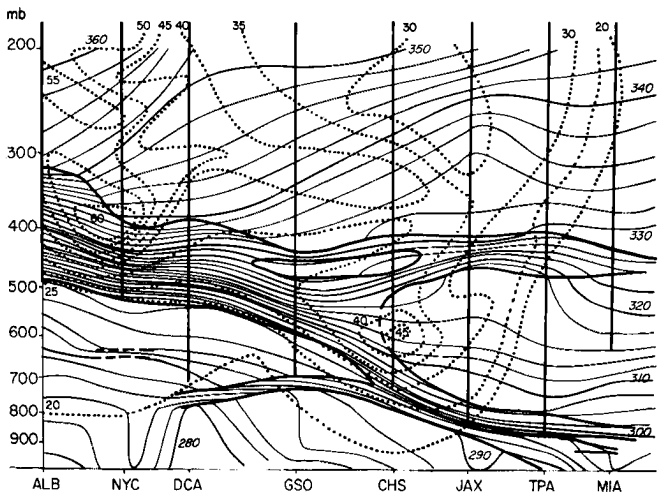

Fig. 9: Cross-section through the atmosphere from Albany (ALB), New York, to Miami (MIA), Florida, 23 November 1962, 00 GCT. Thin lines: potential temperatures (° K, slanting numbers); dotted lines: isotachs (mps, vertical numbers). Heavy lines outline stable regions. Heavy vertical lines over station locations mark the extent of "motorboating" humidity reports.

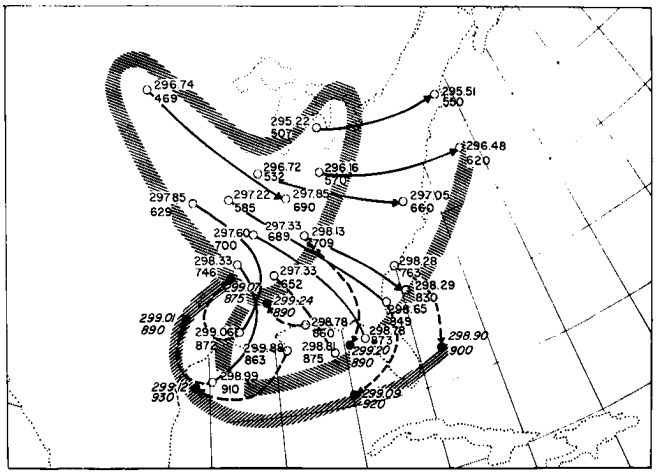

Fig. 10: Trajectories on 295K isentropic surface; from 22 November 1962, 12 GCT, to 23 November 00 GCT: full lines with arrows; from 23 November 00 GCT to 12 GCT: broken lines with arrows. Numerical values of Montgomery stream function (units 10^7 cm^2 sec^{-2}) and of pressure (mb) are given at starting and terminal points of trajectories: vertical figures for the first two map times; slanting figures for 23 November 00 GCT. The centers of the hatched bands indicate the probable boundaries of tropopause air as in Fig. 8.

belts should be considered as area boundaries). Trajectories from 22 November 00 GCT to 12 GCT are dashed and those from 22 November 12 GCT to 23 November 00 GCT are entered as full lines. Values of potential vorticity, Montgomery stream function, pressure and thickness of the dry stable layer are plotted at starting and terminal points of the trajectories as indicated in the plotting model. The general sinking tendency of this air may be recognized from the increasing pressure values along the trajectories. As previously stated most of the sinking occurs along the southern branch of the jet stream with especially rapid vertical motions. This occurs after the split between the two branches has widened and the southern branch curves anticyclonically.

The northern branch continues cyclonically with only slight pressure increases along its trajectories. We may surmise that this branch also carries nuclear debris from the Russian event; although there is no evidence which proves this conjecture other than the common jet maximum from which both branches emanate.

Potential vorticities are reasonably well conserved along the path of the moving air mass, except for the two trajectories ending near Cape Kennedy and near Charleston, South Carolina. These two trajectories originate on 22 November 12 GCT in regions of strong potential vorticity gradients (see Fig. 7). Thus, small errors in analysis may be held responsible for the apparent decreases in P. Changes of Montgomery stream function values along the trajectories are in agreement with observed accelerations and local changes (Danielsen, 1961).

Large discrepancies appear, however, in the values of Δp (pressure thickness of the sinking stable layer) given along the trajectories. Though the flow divergence indicated by the fanning-out of the trajectories would at least in part be compensated by the observed decelerations, the thickness of the stable layer could hardly be expected to increase as the dry air advances. Yet this is

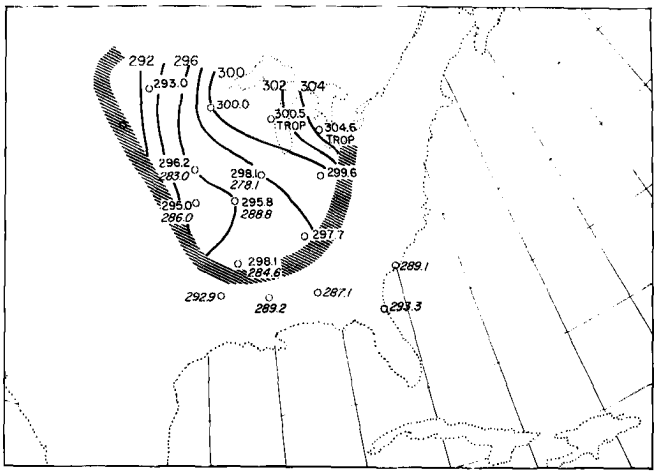

Fig. 11: Isolines of potential temperature (K) of bottom of upper stable layer on 22 November 12 GCT. Outline of tropopause air as in Fig. 8. Vertical numbers give potential temperatures at bottom of upper stable layer, slanting numbers at bottom of lower layer.

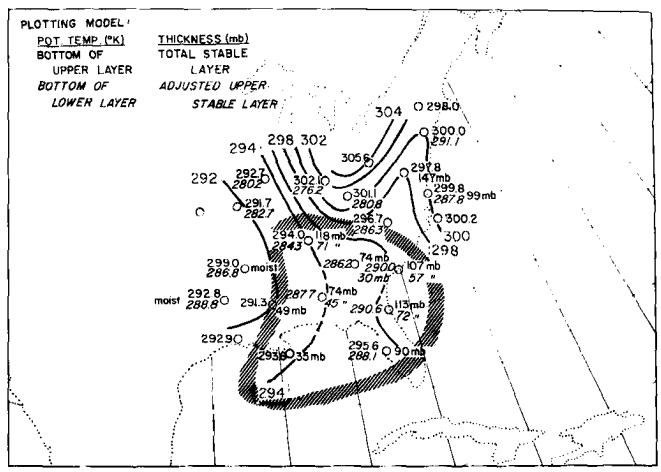

Fig. 12: Isolines of potential temperatures (K) of the bottom of the upper stable layer: solid lines where direct analysis was possible; dashed lines, where interpolation was necessary. Numerical values of potential temperatures: vertical numbers refer to bottom of upper stable layer, slanting numbers to bottom of lower layer. Numerical values of thickness of stable layer (mb). Vertical numbers refer to unadjusted layer (upper layer, where distinction could be made between upper or lower layer; elsewhere: total stable layer); slanting numbers: adjusted thickness of upper layer only. Hatched band encloses air at 23 November 1962 00 GCT, which later is involved in the fallout process.

what it apparently does most drastically in the region characterized by the two aforementioned trajectories. Other trajectories to the west of this area show the expected decrease in Δp, signifying the flattening process which this layer undergoes after extrusion from the tropopause region.

The reasons for this apparently inconsistant behavior of Δp are revealed by the cross-section of Fig. 9. The stable layer containing the isentropic surfaces 300K and 295K - the latter characterizing the bottom of this layer - attaches itself to another stable layer whose lower boundary lies close to 290K. Especially over Charleston (CHS), South Carolina, and Jacksonville (JAX), Florida, the two layers have merged completely, thus accounting for the abnormally high thicknesses in this region (Fig. 8).

There is little doubt that the lower layer is not responsible for the observed radioactive fallout. Let us return for a moment to Fig. 3. The cross-section presented in this diagram corresponds to a location and map time where the downward transport processes had to be well underway, as the subsequent trajectories on the 300K and 295K surfaces demonstrate (Figs. 8 and 10). In Fig. 3 the 290K isentropic surface is contained in a stable layer over Oklahoma City (OKC) and Topeka (TOP). Winds in this layer are light (< 20 mps). It may be seen that the 290K surface stays below the 600-mb level, and is thus indicative of low-tropospheric temperatures. Obviously this layer has been outside the range of jet stream velocities and therefore could not have carried debris of such young age as was observed.

As may be seen from this cross-section (Fig. 3) the stable layer containing 300K is imported from aloft with relatively high wind speeds. At this observation time the upper layer still is completely separate from the lower one. This is also evident from Fig. 11 in which potential temperatures of the bottom of the upper (vertical figures) and lower layer (slanting figures) are plotted. The lower stable layer is already present over a large area of the Central and Southern United States as the upper layer advances. (As before, its boundary

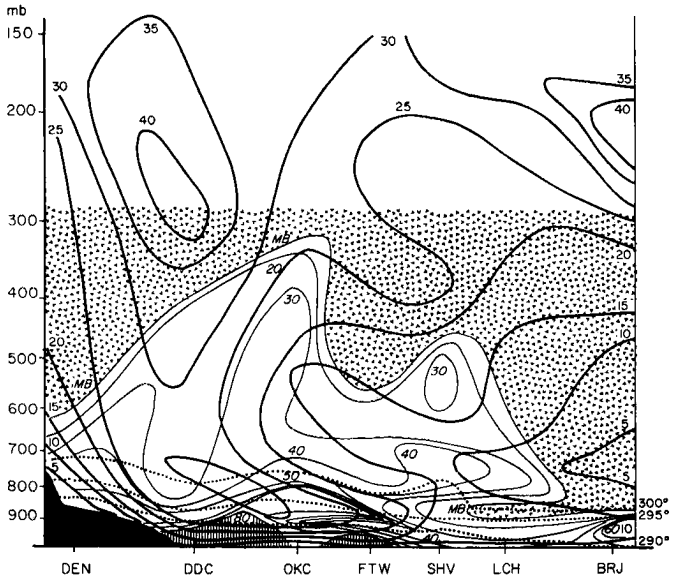

23 November 1962, 12 GCT

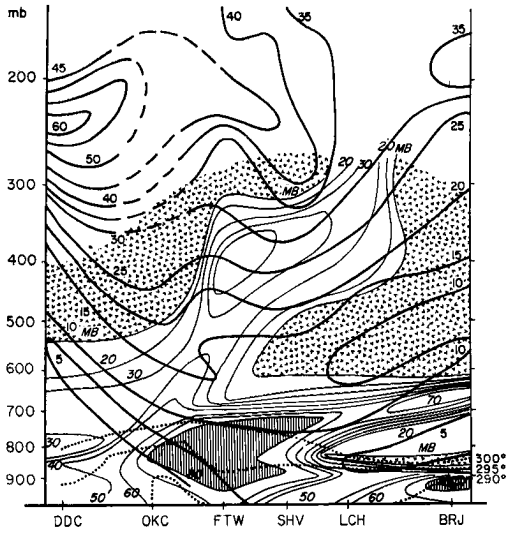

24 November 1962, 12 GCT

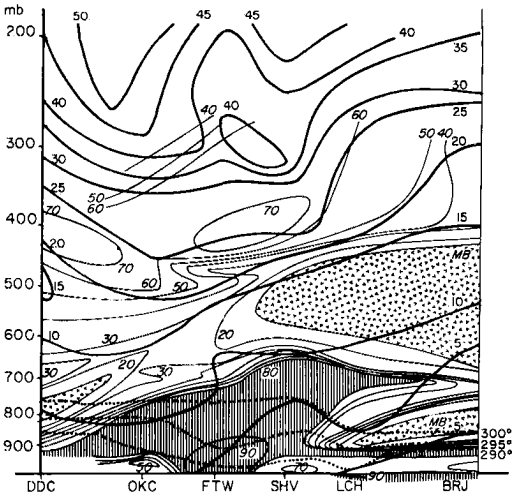

24 November 1962, 00 GCT

Fig. 13: Cross-sections through the atmosphere from Denver (DEN), Colorado, and Dodge City (DDC), Kansas, to Burrwood (BRJ), Louisiana, for observation times as indicated. Heavy lines: isotachs (mps, vertical numbers); thin lines: relative humidities (per cent, slanting numbers); areas with "motorboating" reports and with humidities exceeding 80 per cent are marked by different shading. Dotted lines indicate potential temperatures of 290K, 295K, and 300K.

is indicated by hatching). An analysis of the bottom θ values of the upper layer indicates a reasonably consistant pattern.

In line with the preceding arguments it appears that the upper layer has been superimposed upon a pre-existing lower stable layer in the course of extensive sinking processes. The previous mass transport calculations, based upon the measurements of the thickness of the combined stable layers, should therefore give too high values of stratospheric air import, unless one were able to separate the two layers. This has been attempted with the aid of Fig. 12.

The center of the hatched boundary in this diagram outlines the sinking air mass on 23 November, 00 GCT. Vertical Δp values (in mb) which give thicknesses of the combined stable layers therefore may need adjustment. From those stations in which the upper layer could be distinguished from the lower one, potential temperatures of the bottom of the upper layer could be determined. An interpolation of these potential temperatures of the layer bottom (dashed lines) now permits an estimate of the bottom of the upper layer over those stations where it has become obscured by the lower layer. The adjusted layer thicknesses (in mb) thus obtained are indicated with slanting figures.

In Table III the unadjusted amount of contaminated air which split off the main jet stream has been estimated to be:

$$0.87 \times 10^{12} \text{ metric tons}$$

Elimination of the mass of the bottom layer yields:

$$0.64 \times 10^{12} \text{ metric tons}$$

The original estimate has been too high by approximately 25%. A similar correction should probably be applied to all other values listed in Table III., however, since the separation of the two layers becomes more difficult as the sinking air advances, this could hardly be considered worthwhile. May it suffice, therefore, to state that 0.6×10^{12} metric tons is a fairly reliable order-of-magnitude estimate of the air masses involved in producing the radioactive fallout observed at the ground between 24 and 27 November 1962 over the southern United States.

IV. THE FALLOUT PROCESS

A comparison of Fig. 10 with Fig. 8 shows that the dry air masses contained within the stable layer move in essentially the same way on both isentropic surfaces. There is an indication of slightly more anticyclonic curvature on the 295K surface than on the higher one. Trajectories of selected points between the first two observation times are shown by solid lines and between the latter two observation times by dashed lines. Montgomery stream function (in units 10^7 cm^2 sec^{-2}) and pressure values (mb) are plotted for starting and terminal points of trajectories (vertical figures for the first two observation times, slanting figures for 23 November 12 GCT). As may be seen from these values, some portions of the layer are sinking as fast as 200 mb and more within 12 hours (corresponding to ca. 3 km/12 hours or 7 cm/sec). Sinking rates are decreasing sharply as the air becomes a part of the quasi-stationary anticyclonic system. This appears to happen between 23 November 00 and 12 GCT, especially in the region west of Alabama.

To trace isentropic trajectories beyond 23 November 12 GCT would have been meaningless. Wind speeds had decreased by that time and diabatic effects had started to become quite effective.

Fig. 13 shows a series of cross sections from Burrwood (BRJ), Louisiana, to Dodge City (DDC), Kansas, and to Denver (DEN), Colorado. These sections are approximately oriented along the inflow of dry air in the stable layer. "Motorboating" reports and relative humidities in excess of 80% have been indicated by different shading.

On 23 November 12 GCT the air above 500 mb is generally dry. A moderately moist tongue over Dodge City (DDC) and Oklahoma City (OKC) overlies the low level jet stream (see also Fig. 2). A deep dry layer is found over Burrwood (BRJ). Its upper portion is associated with a weak subtropical jet stream. The lower portions of this dry air have been imported, however, from the north, as is clearly evident from Figs. 2, 8 and 10. A rather shallow tongue of dry air extends along the 295 and 300K surfaces. Lake Charles (LCH), Louisiana, reports "motorboating" at these potential temperature levels, and relatively dry air is present as far west as Fort Worth (FTW), Texas.

If no diabatic processes were active we should expect this dry tongue to proceed westward at a speed as indicated by the isotachs in Fig. 4. This is not the case, however. The dry layer is found at the same location on 24 November 00 GCT and has even receded slightly by 24 November 12 GCT. At the same time a large import of moist air from

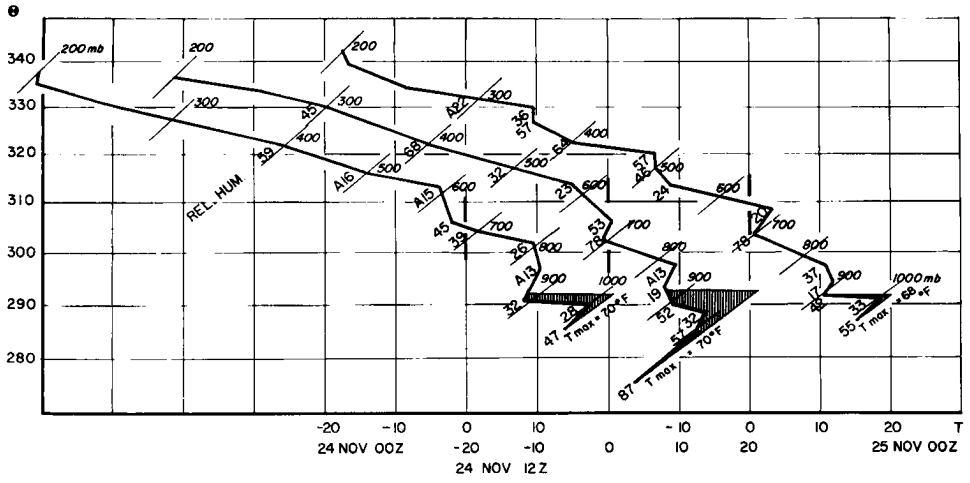

Fig. 14: Temperature soundings at Jackson, Mississippi on 24 November 1962, 00 and 12 GCT, and on 25 November 00 GCT, plotted on a tephigram. Soundings have been shifted by 20° C along the temperature coordinate for successive observation times. Relative humidities are plotted along soundings (maximum humidities possible with "motorboating" are prefixed with letter "A"). Standard pressure levels along sounding are indicated by short lines and are labelled with small slanting numbers. The adiabat through the observed surface temperature maximum is assumed to determine the depth of the adiabatic mixing layer (marked by hatching).

the Gulf of Mexico is evident, especially over Fort Worth (FTW). Fig. 1 indicates precipitation in this region on 24 November.

According to Figs. 5 and 6, the dry air over Lake Charles at 295K was encountered near 900 mb on 23 November 12 GCT. The saturation mixing ratio thus is seen from a tephigram to be approximately 10.8 g/kg. The maximum mixing ratio for "motorboating" may be assumed to be 1.4 g/kg. (Actual values may have been considerably below this value). A 295K trajectory calculated from Fig. 4, beginning at the leading edge of the "motorboating" layer on 23 November 12 GCT, is found to be halfway between Shreveport (SHV), Louisiana, and Fort Worth (FTW), Texas after 12 hours. According to Figs. 5 and 13, relative humidities have gone up to approximately 80% in this region. Mixing ratios, therefore, are now 8.6 g/kg.

Let us make the bold assumption that this mixing ratio value has been produced by mixing dry contaminated air imported along the previously described trajectories (maximum mixing ratio 1.4 g/kg) with saturated air advancing from the Gulf of Mexico and "tapping" the dry layer from below (saturation mixing ratio for this pressure level and temperature 10.8 g/kg). To arrive at the mixing ratio observed on 24 November 00 GCT dry and saturated air would have to be mixed at a ratio of 3 to 10. While these figures should only be taken as a very crude estimate, they still indicate that strong vertical mixing must take place to prevent the dry layer from advancing any further.

The fallout in the precipitation region observed on 24 November 15 GCT and on the subsequent days may be explained, therefore, by such mixing processes. The layer which carried the nuclear debris advanced well within the reach of the mixing layer

near the ground. The surge of moist air observed in the cross-sections of Fig. 13 eventually eliminated the dry contaminated layer altogether as is already indicated from the cross-section of 24 November 12 GCT.

For stations outside the precipitation region reporting high fallout concentration, downward mixing must also be held responsible for the observed values. As soon as the contaminated layer is tapped by the adiabatic layer generated during the period of diurnal heating, nuclear debris will be carried downward by turbulent processes. The soundings of Jackson, Mississippi, illustrate this process very well (Fig. 14). The dry adiabat drawn through the maximum temperature as reported in the "Daily Weather Map" of the U.S. Weather Bureau may be taken as an indication of the top of the mixing layer. According to these soundings, part of the dry layer is evidently eroded by diurnal heating and resulting mixing processes.

V. FORECASTING OF FALLOUT

In the foregoing the processes were described which lead to the observed fallout maximum over the southern United States between 24 and 27 November 1962. Such vertical transport processes should be expected with any jet stream system of low or high latitudes which shows a sufficiently distinct vorticity pattern produced by wind shear and/or streamline curvature, and which gives strong divergence and convergence patterns according to

$$\frac{dQ}{dt} = -DQ \qquad (5)$$

(Q is the vertical component of absolute vorticity, D stands for the horizontal divergence). Stratospheric - tropospheric mass exchange should therefore be expected near the subtropical jet stream (STJ) as well as near the polar front (PFJ) or arctic front (AFJ) jet.[2]

If we introduce the restrictive requirement that such transport processes through the jet stream should reach the ground in a relatively short time, we have to consider that the troposphere below the 500 mb level is nearly barotropic underneath the subtropical jet stream. On the other hand baroclinic zones are found to stretch throughout the troposphere under certain parts of the PFJ. Transport processes associated with the latter type of jet stream are therefore confined to narrower and better defined regions, and should be expected to reach through deeper portions of the troposphere that with the STJ. Moreover, the STJ occurs at levels of potential temperatures much too warm to be found near the ground.

Near the PFJ we find that cold temperatures characteristic of the low tropopause to the north of the jet axis correspond to nearly the same potential temperature as may be found in "subsidence inversions" of strong anticyclones near the ground. A direct quasi-adiabatic mass transport from the tropopause region or the lower stratosphere to such inversions above the friction layer should therefore be possible in a matter of approximately two days, as the past case histories proved.

The margin of potential temperatures at which such rapid downward transport processes may operate along an isentropic surface seems to be quite small. If the potential temperatures of a stable baroclinic zone are too low, the air contained within could not have been of stratospheric origin unless diabatic cooling processes-active over some period of time - could be postulated. If, on the other hand, the potential temperatures in such a layer are too high, the air contained within the layer may be of stratospheric origin. It could not reach the ground, however, without the action of diabatic cooling processes.

This limitation on potential temperatures does not necessarily apply to debris encountered by aircraft or balloons in the upper troposphere. Here quite sharp increases in radioactive contamination may be observed at potential temperatures higher than encountered near the ground (Danielsen, 1964). If such layers were eventually to reach the ground, they must undergo radiative cooling and mixing. With the action of such diabatic processes it should be expected that the increases in fallout eventually observed near the ground would be diffused over a relatively wide area.

The cases of fallout studied so far, on the other hand, were characterized by well defined fallout regions of relatively small extent with radiation levels well above the seasonal and re-

---

[2]Because AFJ and PFJ show nearly the same structural characteristics, the designation PFJ will be used throughout the following discussion, irrespective of the two airmasses to whose temperature contrast the jet stream is attached.

TABLE IV. Characteristic potential temperatures of layers containing concentrated radioactive fallout reaching the ground

Date of Fallout	Location	Isentropic surface followed within contaminated stable layer	Age of Debris	Remarks	Reference
17-21 Sept. 1961	Southeast USA	298K and 303K	ca. 8 days	Debris layer also encountered by balloon over Flin Flon, Canada, on 14 and 15 Sept. 1961	Reiter (1963a, b) Anderson (1962)
30Mar-2 Apr. 1963	Western, USA	300K	>100 days	Test Ban Treaty in effect	Mahlman (1964)
24-27 Nov 1962	Southern USA	295 and 300K	< 15 days	Dry fallout combined with local wash-out	

gional background. Rapid quasi-adiabatic vertical transport processes should therefore be held responsible for the observed increase of dry fallout near the ground.[3]

With what has been said about the restriction on potential temperatures at which such adiabatic transports may occur, Table IV may be interpreted as characterizing conditions at least during the period from autumn through spring. From this table we may conclude that only jet streams whose "jet stream front" contain potential temperatures in the order of 295 to 305K could be instrumental in bringing contaminated stratospheric or tropopause air to the ground in a quasi-adiabatic "surge" confined to a relatively small area.

If this conclusion were to hold true in additional case studies of similarly concentrated fallout events, it could be used effectively in fallout forecasting. If such a stable layer containg these potential temperatures were advected over a region of anticyclogenesis, the horizontal mass divergence from this region should soon bring the layer into contact with the adiabatic ground layer. Sinking rates of approximately 200 mb per 12 hours as indicated by Fig. 10 are well within the realm of observations.

An effective short and medium range forecasting model for fallout of low stratospheric origin should, therefore, incorporate a search of the "jet stream front" at the 400 mb level for the potential temperatures indicated above, together with well pronounced cyclogenesis and vorticity advection at this level. More tests will have to be conducted in order to determine the effectiveness of such a forecasting procedure.

VI. THE EFFECT OF JET STREAMS ON STRATOSPHERIC - TROPOSPHERIC MASS EXCHANGE

Both Mahlman's (1964) and the foregoing estimates of the amount of stratospheric or tropopause air transported into the mixing layer near the ground arrive at the same order of magnitude. Assuming this to be a value of transport typical for a jet maximum of average intensity, we may make a rough estimate of the effect of such jet stream systems on the interchange of stratospheric and tropospheric air.

[3]Wet fallout processes, in general, should not be included in this consideration, although they may also lead to well defined areas of high radioactivity concentration. With the moist-adiabatic processes involved in such cases, contaminated layers at high potential temperatures may be tapped, and their debris may be brought to the ground by falling precipitation.

Assuming the average tropopause pressure to be 200 mb (2×10^5 dynes cm^{-2}) at an approximate mean height of 12 km, the area covered by the tropopause would be 51.1×10^7 km^2, and the total mass of stratospheric air would be approximately 1.04×10^{21} grams (assuming a value of 980.6 for the acceleration of gravity), or 0.52×10^{21} grams for one hemisphere.

The estimated transport of 0.6×10^{18} grams accomplished by an average jet stream system, therefore, accounts for a little over 0.1% of the total stratospheric air in one hemisphere. If we assumed five such waves to be active around the hemisphere at the same time, about 0.5 per cent of stratospheric air would be transported to the ground.

Libby (1959) estimates the average residence time of stratospheric air to be 5 years for equatorial latitudes and less than one year for polar latitudes. Since the latter cover less than one third of the area of one hemisphere, the transport processes described above would carry approximately 1.5 per cent of polar stratospheric air to the ground.

As described in the foregoing sections, this estimate covers only processes which carry stratospheric air to the ground in a matter of very short time (approximately 2 days) and under nearly adiabatic conditions. However, an even larger portion of air that has come out of the stratosphere on the 295K, 300K, and higher potential temperature surfaces follows the northern jet stream branch after the split, and does not sink to the ground immediately. Furthermore, similar exchange processes should be expected near the subtropical jet stream without even reaching the ground directly in quasi-adiabatic motion. For hemispheric processes transporting polar and mid-latitude stratospheric air through the tropopause gap near jet streams, irrespective of the time in which it reaches the ground, one might therefore increase the above per cent estimate by as much as a factor of five. One such period per month of wave formation along the hemispheric polar-front and subtropical jet-streams, causing pronounced vorticity patterns and consequent vertical motions, could thus account for most of the stratospheric tropospheric mass transport postulated by Libby.

VII. THE LOW LEVEL JET STREAM (LLJ) IN ISENTROPIC ANALYSIS

By Figs. 2 and 4 the life cycle of a LLJ is described. Its first indications appear on 22 November 12 GCT over Grand Junction, Colorado, and Salt Lake City, Utah, well to the west of the Continental Divide. Southerly wind velocities in this low-level current have not yet reached jet-stream intensities at this time. Nevertheless, the change in flow pattern from the preceding map time is quite significant. An import of moist air seems to be associated with this incipient jet stream (Fig. 5). It blows across a quasi-stationary surface front along which subsequently a cyclone develops.

It is of interest to note that the origin of a LLJ does not have to lie east of the Rocky Mountains. While the orographic configuration certainly may have favored its intensification, its incipient stage occurred west of the highest mountain ranges.

Apparently this jet stream starts as a very shallow phenomenon. The 22 November 12 GCT charts show it on the 295K surface (Fig. 4) but not yet on the 300K surface (although even on this level, weak southerly winds are indicated) (Fig. 2). On 23 November 00 GCT the LLJ is already clearly established: as a separate isotach maximum ahead of the frontal system on the 295K surface; as a branch merging into the main jet stream on the 300K surface.

Fig. 6 indicates the general ascending motions associated with the LLJ. In view of the moisture imported by this jet, and in view of observed cloudiness and precipitation (Fig. 1), we have to assume that the air will not travel isentropically. Nevertheless, Figs. 2 and 4 may be taken as a good qualitative indicator of the behavior of the LLJ.

The LLJ reaches peak intensities on 23 November 12 GCT while it still is a low tropospheric phenomenon (see Fig. 13). The subsequent maps show this jet stream to merge with the main jet in the upper troposphere.

From these analyses it appears that the LLJ is not an entity which stands separate from the other jet stream systems at tropopause level. Such erroneous assumptions have only been derived from the indiscriminate use of isobaric analyses. These, of course, would show an isolated wind maximum at the 850 or the 700-mb level, which is seemingly unrelated with the jet stream at 300 mb. Isentropic analysis, however, reveals that the LLJ constitutes a channelled inflow of air into the upper tropospheric jet-stream circulation, thus actually being a branch of the latter.

From Fig. 5 it may be seen, that the import

of moist air associated with the LLJ apparently cuts off the dry and contaminated air supply which leads to the observed fallout. This inflow of moist air aloft, prompted by the anticyclonic circulation in which the contaminated air is caught, may help to explain the fact that fallout from stratospheric air reaching the ground occurs in discrete "surges" and not as a continuous "trickle". Such moist air inflow does not necessarily have to be associated with jet-stream velocities, however. A rather broad anticyclonic flow, as was observed during the case of September 1961 (Reiter 1963a, b), may have the same effect.

VIII. CONCLUSIONS AND OUTLOOK

The foregoing case study of radioactive fallout showed that contaminated air from the tropopause region or from the lower stratosphere may traverse the whole depth of the troposphere in a matter of approximately two days. It does so quasi-adiabatically while contained within a relatively shallow stable layer.

The narrow range of potential temperatures within which stratospheric air may pass directly and quasi-adiabatically to the ground allows only polar front and arctic front jet streams with distinct vorticity patterns to play a major role in this type of rapid transport processes. Since such vorticity patterns are commonly found during periods of increased cyclogenesis and anticyclogenesis, indications of the latter could provide short and medium range forecasting possibilities on a hemispheric basis.

Not all the air involved in the mixing process through the "tropopause gap" actually reaches the ground. A large portion of it branches off and follows the course of the main jet stream at upper and mid-tropospheric levels. The assumptions made in Chapter 6 on the amount of air that remains aloft in the indicated fashion should be considered as conservative. More research will have to be carried out to determine its actual proportions.

For local fallout predictions the splitting of the jet stream (analyzed on an isentropic surface) may serve as a first clue. It is not, as yet, fully understood what causes this split. Hydrodynamic instability observed in the region where the split occurs may play a certain role.

Of the stratospheric-tropospheric mass interchange processes only those associated with sinking motion have been studied so far. It is conceivable that the jet stream constitutes an equally powerful source of return flow of tropospheric air into the stratosphere. These freshly imported air masses are expected to mix with originally stratospheric air, thereby lowering the concentration of stratospheric radioactive debris at those levels and in these regions where this inflow occurs.

Since this return flow would at least in part be moist-adiabatic, computation of trajectories will be very complex. An airborne measurement program geared to measure atmospheric properties characteristic of tropospheric air at higher levels (e.g. water vapor, radioactive elements of the radium family, etc.) would enhance greatly our understanding of the full nature of atmospheric transport processes through the tropopause level and of the mixing processes in the stratosphere.

IX. ACKNOWLEDGEMENTS

The authors are indebted to Messr. Donald W. Beran, William E. Davis and Gene L. Wooldridge for their assistance in technical computations. Mr. William D. Ehrman helped in the preparation of the raw data. Mrs. Viola Weiland typed the manuscript.

REFERENCES

Anderson, K.A., 1962: Thin atmospheric layers of radioactive debris during September 1961, Cosmic Ray Group, Department of Physics, University of California, Berkley, Scientific Report to ONR, 23 pp.

Arakawa, H., 1941: Stabilitats - und Boigkeitsbedingungen der allegemeinen Zirkulation der Atmosphare, Meteorologische Zeitschrift, Braunschweig, 58, 381-384.

_____, 1942: Stabilitatskriterien der atmosphharischen horizontalen Turbulenz, Gerlands Beitrage zur Geophysik, Leipzig, 58, 3-10.

_____, 1951: Possible heavy turbulence exchange between the extratropical tropospheric air and the stratospheric air, Tellus, 3, 208-211.

Danielsen, E.F., 1959: The laminar structure of the atmosphere and its relation to the concept of a tropopause, Archiv für Meteorologie, Geophysik und Bioklimatologie, Serie A, 11, 293-332.

Danielsen, E. F., 1961: Trajectories: isobaric, isentropic, and actual, Journal of Meteorology, 18, 479-486.

_____, 1964: Radioactivity transport from stratosphere to troposphere, Pennsylvania State University Mineral Industries, 33(6): 1-7.

_____, and E. R. Reiter, 1960: Bemerkungen zu E. Kleinschmidt: Nicht-adiabatische Abkühlung im Bereich des Jet-Stream, Beiträge zur Physik der Atmosphäre, 32(3/4), 265-273.

Endlich, R. M. and G. S. McLean, 1957: The structure of the jet stream core, Journal of Meteorology, 14, 543-552.

Kao, S. K. and W. P. Hurley, 1962: Variations of the kinetic energy of large-scale eddy currents in relation to the jet stream, Journal of Geophysical Research, 67, 4233-4242.

Kleinschmidt, E. Jr., 1941a: Stabilitatstheorie des geostrophischen Windfeldes, Annalen d. Hydrogr. Berlin, 69, 305-325.

_____, 1941b: Zür Theorie der labilen Anordnung, Meteorologische Zeitschrift, Braunschweig, 58, 157-163.

_____, 1959: Nicht-adiabatische Abkuhlungen im Bereich des Jetstream, Beiträge zur Physik der Atmosphäre, 32 (1/2), 94-108.

Libby, W. F., 1959: Radioactive fallout particularly from the Russian October series, Science 45, 151-175.

Mahlman, J. D., 1964: Relation of stratospheric-tropospheric mass exchange mechanisms to surface radioactivity peaks, Atmospheric Science Technical Paper No. 58, Colorado State University,

Murgatroyd, R. J., 1959: Jet stream flight of 6th March, 1959, Unpublished Report.

Reed, R. J. and E. F. Danielsen, 1959: Fronts in the vicinity of the tropopause, Archiv für Meteorologie, Geophysik ünd Bioklimatologie, Series A. 11, 1-17.

Reiter, E. R., 1961a: Meteorologie der Strahlströme (Jet Streams), Vienna, Springer, 473 pp.

Reiter, 1961b: Project Jet Stream research flight No. 30, April 1957, Quarterly Journal of the Royal Meteorological Society, 87, 332-345.

_____, 1961c: The detailed structure of the wind field near the jet stream, Journal of Meteorology, 18, 9-30.

_____, 1962: Die vertikale Strüktur des Strahlstromkernes aüs Forschüngsflügen des Project Jet Stream, Berichte d. Deutsch. Wetterd, No. 80.

_____, 1963a: A case study of radioactive fallout, Atmospheric Science Technical Paper No. 42, Colorado State University, 35 pp.

_____, 1963b: A case study of radioactive fallout, Journal of Applied Meteorology, 2, 691-705.

_____, 1963c: Jet Stream Meteorology, Chicago, University of Chicago Press, 513 pp.

_____, 1963d: Note on the eddy kinetic energy distribution in relation to the jet stream, Journal of Geophysical Research, 68, 1785-1787.

_____, 1964: Comments on paper by S. Penn and E. A. Martell, "An analysis of the radioactive fallout over North America in late September 1961", Journal of Geophysical Research, 69, 786-788.

Saucier, W. J., 1958: A summary of wind distribution in the jet streams of the Southeast United States investigated by Project Jet Stream, Department of Oceanography and Meteorology, Texas A & M, Final Report, AF 19 (604-1565) pp 6-57.

Staley, D. O., 1960: Evaluation of potential vorticity changes near the tropopause and the related vertical motions, vertical advection of vorticity, and transport of radioactive debris from stratosphere to troposphere, Journal of Meteorology, 17, 591-620.

Staley, D. O., 1962: On the mechanism of mass and radioactivity transport from stratosphere to troposphere, Journal of the Atmospheric Sciences, 19, 450-457.

U. S. Atomic Energy Commission, 1964: Health and Safety Laboratory, Fallout Program Quart. Summ. Rep., Jan 1, 1964, HASL-142.

Van Mieghem, J., 1944a: Forme intrinseque dü critere d'instabilite dynamique de E. KLEINSCHMIDT, Bull. Acad. Belg. Cl. Sci., ser. 5, 30, 19-33.

Van Mieghem, J., 1944b: Relation d'identite entre la stabilite de l'equilibre dynamique de E. KLEINSCHMIDT et la stabilite des oscillations d'inertie de l'atmosphere terrestre. Bull. Acad. Belg. Cl. Sci., ser. 5, 30, 134-143

DEBRIS SOURCE OF THE HEAVY FALLOUT OVER SOUTHERN UNITED STATES ON 24-27 NOVEMBER 1962

by

J. D. Mahlman and William E. Davis

ABSTRACT

Reiter and Mahlman (1964) have investigated a case of heavy radioactive fallout observed over the south central United States between 24 and 27 November 1962. Their conclusion that this debris might have had its source in an atmospheric test near Semipalatinsk, U. S. S. R., on 17 November 1962 is corroborated by means of isobaric trajectory computations.

I. INTRODUCTION

The physical processes leading to the presence of intense radioactive fallout beginning 24 November 1962 over the south central United States were investigated in detail by Reiter and Mahlman (1964). The measured debris ages in the fallout region were less than 15 days with individual measurements as low as 9 days. A comparison of these debris ages with known atmospheric nuclear tests pointed to a 17 November low-yield detonation at Semipalatinsk, U. S. S. R., as the probable source of the observed radioactivity (see Table I, Reiter and Mahlman, 1964).

Analysis of this case revealed that the fallout increase was due to the presence of a low-level contaminated stable layer which was eventually dissipated by convective motions from below, with and without precipitation. The trajectories of this layer were traced backward in time by the isentropic method. They showed that the layer was associated with cyclogenetic activity at tropopause level and winds of jet stream intensity.

On 22 November 00 GMT the leading edge of this sinking layer was located at 459 mb over Rapid City, South Dakota (662). Another 12 hour isentropic trajectory can be traced back from this point

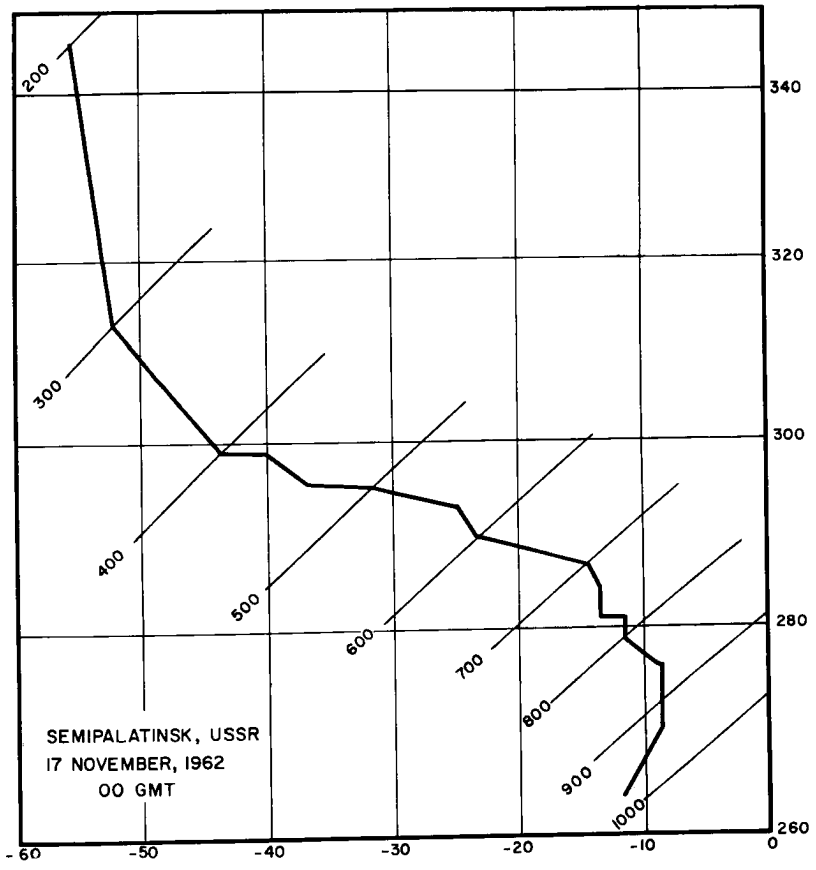

Fig. 1: Temperature sounding at Semipalatinsk, U. S. S. R. on 17 November 1962, 00 GMT, plotted on a tephigram. Horizontal coordinate is temperature, vertical coordinate is potential temperature, and the diagonal lines are pressure.

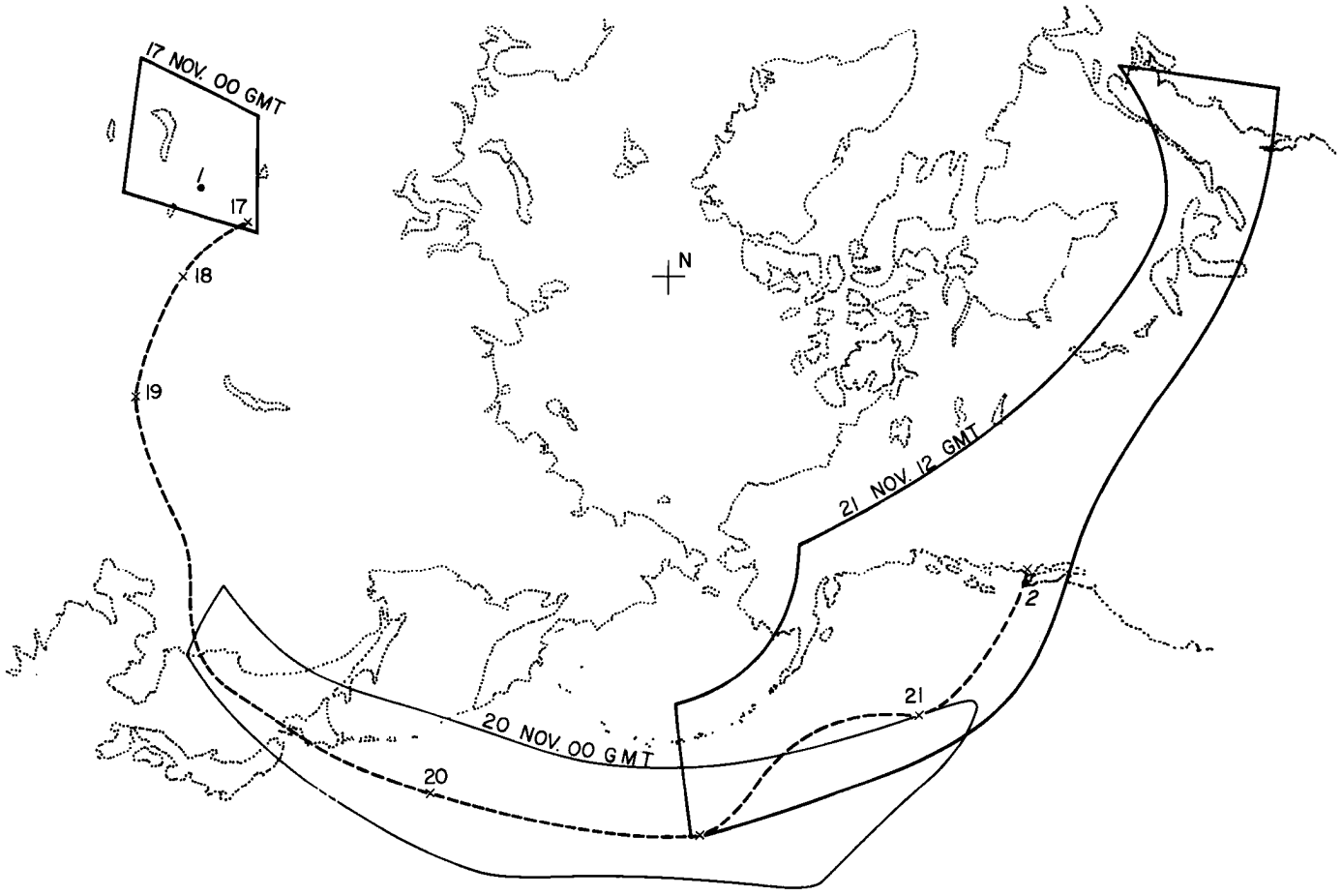

Fig. 2: Area trajectory locations for indicated dates (solid lines) calculated on the 400 mb surface from 17 to 21 November 1962. Quadrilateral enclosing original debris cloud is shown on left side of diagram. Dashed line gives backward point trajectory taken from Port Hardy, Canada region. Location of Semipalatinsk, U.S.S.R., and Port Hardy, Canada, are marked by a "1" and a "2" respectively.

to a region 60 nautical miles northeast of Port Hardy, Canada, and at a pressure of 400 mb.

With the results of these backward trajectories in mind, it was investigated whether or not the explosion of 17 November 1962 at Semipalatinsk, U.S.S.R., could have been a source of the observed debris. This was accomplished by following the possible forward paths of the debris from the Semipalatinsk explosion and by tracing the path of the contaminated layer still further backward in time from the region of heavy fallout.

II. METHOD OF APPROACH

The 17 November nuclear detonation at Semipalatinsk was a comparatively low-yield shot (Table 1) and thus could not have penetrated far into the stratosphere (Machta, List, and Telegadas, 1961). Inspection of the 17 November 00 GMT sounding for Semipalatinsk reveals that a moderately stable layer is present between the 400 mb (potential temperature θ = 299K) and the 300 mb (θ = 312K) surfaces (Fig. 1). This stable layer would exert a damping influence on the bomb-produced thermal convection and therefore trap at least a portion of the debris cloud.

The θ values which define the boundaries of this stable layer are in qualitative agreement with the characteristic potential temperatures of the contaminated layer observed in connection with the 24 November fallout increase over the United States. In order to reliably determine the resultant movement of the Semipalatinsk debris, the best approach would be to employ the isentropic method described by Danielsen (1961). However, this approach appeared to be unfeasible because of the inadequate radiosonde station density over the Pacific Ocean. Therefore, isobaric trajectories had to be substituted for the isentropic method. This proved to be satisfactory as long as no pronounced temperature advection is observed along the trajectory path, so that vertical motions could be assumed negligible.

Because of the uncertainty of time and position of the Semipalatinsk detonation, the trajectories had to be initiated from an area large enough to enclose the unknown debris position, rather than to compute a trajectory from a single initial point. Furthermore, the movement of the debris from this region were complicated by the presence of a rapidly dissipating cut-off cyclone on 17 November. In order to compensate for these uncertainties, a quadrilateral was constructed over the Semipalatinsk area which was large enough to enclose all possible motions of the debris cloud between 17 and 18 November (Fig. 2). The movement of this area was then traced by calculating a series of trajectories from points within the selected quadrilateral. Instead of calculating these point trajectories to ascertain the most probable final positions, the computations were performed so that the uncertainties of the final trajectory positions were also included in the final area - determined by the envelope of the terminal points of the trajectories.

III. MOVEMENT OF THE DEBRIS CLOUD

By utilizing the method outlined in the previous section, the trajectories of the points contained within the selected quadrilateral were calculated at the 400 mb and the 300 mb surfaces. As the area moved eastward, quite pronounced cold air advection was observed on 19 November west of Japan. Because of the possibility that some of the debris may consequently have sunk as low as 500 mb, the area traced on the 400 mb level was superimposed on the 500 mb surface so that isobaric trajectories could also be computed for this lower level. However, by 21 November the 500 mb area was still located over the Pacific Ocean. Hence, it appears that if debris were transported at this level it could not have produced the observed fallout over the southern United States.

The areas traced on the 300 mb and 400 mb surfaces, on the other hand, had reached North America by 21 November 12 GMT (Fig. 2). The trajectories traced backward from the region of fallout to the vicinity of Port Hardy on 21 November 12 GMT, indicate that Semipalatinsk debris could account for the observed fallout increase.

In order to check the validity of this observation, a 400 mb trajectory was traced backward from the Port Hardy region on 21 November 12 GMT (Fig. 2). On 17 November this trajectory was seen to be located within the originally selected quadrilateral over Semipalatinsk.

These trajectory analyses reveal that the Semipalatinsk nuclear detonation of 17 November 1962 provided the probable source of the heavy fallout measured over the south central United States on 24-27 November. Thus, the conclusion reached by Reiter and Mahlman (1964) as to the source of this heavy fallout appears to be justified.

REFERENCES

Danielsen, E. F., 1961: Trajectories, isobaric, isentropic and actual, Journal of Meteorology, 18, 479-486.

Machta, L., R. J. List, and K. Telegas, 1961: An interpretation of global fallout, In: Radioactive Fallout from Nuclear Tests, Proceedings of a Book 1, 149-169.

Reiter, E. R. and J. D. Mahlman, 1964: Heavy fallout over the southern United States in November 1962, In: Technical Paper No. 58, Department of Atmospheric Science, Colorado State University.

ON THE FEASIBILITY OF RELATING SEASONAL FALLOUT OSCILLATIONS TO HEMISPHERIC INDEX PATTERNS

by

J. D. Mahlman

ABSTRACT

The downward transport of radioactive debris from the stratosphere -- in association with tropopause - level cyclogenesis -- may serve as a possible physical explanation of the spring fallout peaks. It is suggested that an index be derived which measures the relative amount of cyclonic activity in the atmosphere, thus permitting an evaluation of the possible interaction between these two phenomena.

ON THE FEASIBILITY OF RELATING SEASONAL FALLOUT OSCILLATIONS TO HEMISPHERIC INDEX PATTERNS

In virtually every year since about 1955 a spring maximum of surface radioactivity resulting from nuclear testing has appeared in the northern hemisphere (Fry, Jew, and Kuroda, 1960; Gustafson, Brar, and Kerrigan, 1961; Peirson, 1963) (Figs. 1 and 2). This spring maximum is one which is distinct from the heavy fallout which is observed to follow immediately after periods of heavy testing in the atmosphere. The fallout maxima which occur immediately after these testing periods are in accordance with the assumption that the mean tropospheric residence time of radioactive debris is of the order of one month. Because the spring peaks often occur many months after the termination of atmospheric nuclear testing, it is necessary to postulate that the stratosphere provides the debris source for these maxima (Fry, Jew, and Kuroda, 1960; Libby and Palmer, 1960).

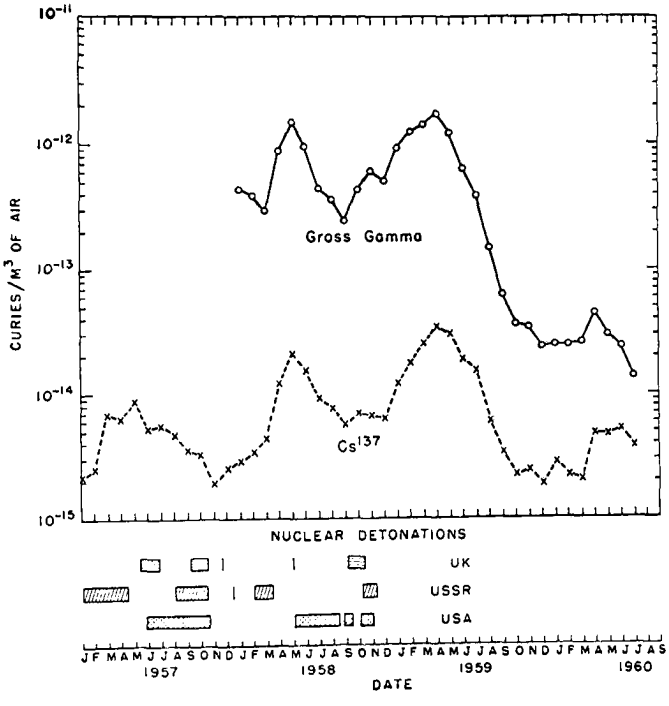

Fig. 1: Concentration of fission products in surface air at Argonne National Laboratory (Gustafson, Brar, and Kerrigan, 1961).

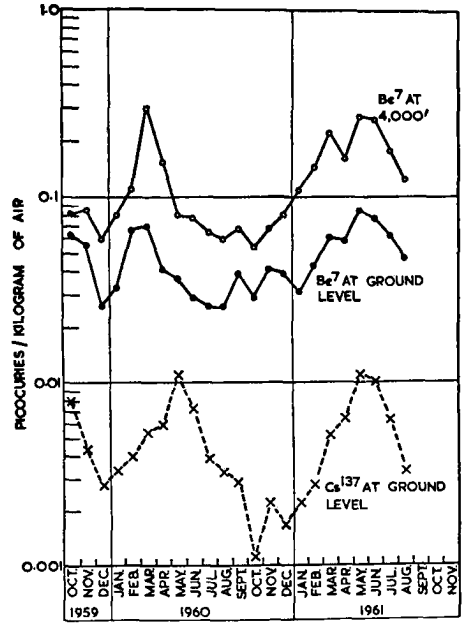

Fig. 2: Seasonal concentration of beryllium-7 and cesium-137 in μμ curies (picocuries) per kilogram of air over Great Britain (Peirson, 1963).

Because of the higher static stabilities and lack of precipitation scavenging in the stratosphere one would expect much longer particle residence times in this region. At present the most plausible estimate of mean residence time is five years for the tropical stratosphere and one year or less for the polar stratosphere (Libby, 1959). It is thus reasonable to assume that the stratosphere is the probable debris source for these seasonal oscillations in surface fallout intensity.

With this assumption the problem of explaining the seasonal fallout variations now becomes one of understanding the physical processes which lead to an exchange of mass between the stratosphere and troposphere. It has been suggested by several authors that the transport of mass and radioactive debris downward from the stratosphere is associated with extratropical cyclones (Storebø,

1959, 1960; Miyake et al., 1962). Staley (1960) shows that this type of mass exchange occurs as a discrete intrusion and hence results in the transport of large amounts of contaminated air into the troposphere. It has been further hypothesized that the sinking is associated with the cyclogenetic process at tropopause level and leads to the occurrence of individual surface fallout peaks (Mahlman, 1964). More recent research (Reiter and Mahlman, 1964) has in part verified this hypothesis and also revealed that this sinking process is characterized by extremely strong vorticity advection and mass convergence.

Because of the apparent dependence of individual fallout maxima upon upper tropospheric cyclones one may inquire whether the fluctuations in mean seasonal fallout are thus a result of yearly changes in cyclonic activity. A way to examine this would be to develop an index parameter which describes the relative amount of cyclonic activity in the atmosphere and compare its seasonal variation with that of the mean fallout intensity.

Because extratropical disturbances strongly influence the direction of the tropopause-level wind field, it seems advisable to develop an index parameter which is determined by the deviation of the mean wind vector from straight westerly flow and is not dependent upon the pressure field. A non-dimensional index parameter of this form has been developed which arbitrarily assigns a value of 1.0 for straight zonal flow and 0.0 for a pure meridional current. It has been extensively tested by computing daily hemispheric values around a latitude band on the 300 millibar surface. A complete derivation and description of this index method will be included in a later paper. Statistical analysis has revealed that the resultant time series provides a significant indication of the relative amount of cyclonic activity in the atmosphere.

Preliminary comparisons of the index sequence from October 1962 to July 1963 with the mean radioactive fallout for that period has shown a great deal of promise. It appears, at least from this limited set of data, that a correlation exists between the amount of decrease of index over a particular time interval and the mean fallout intensity a few days later. However, the data sample is not sufficiently large to make a conclusive statement at this time.

A more detailed continuation of this approach could conceivably lead to a greater amount of insight into the physical processes which produce both short term and annual fallout variations. For example, the spring fallout peaks might be due to a "tapping" of a debris source in the lower stratosphere by increased cyclonic activity during this time of year. These peaks might also be a result of seasonal variations of the vertical and horizontal mass transport processes in deep layers of the stratosphere, thus producing a non-constant debris source above the tropopause (Libby and Palmer, 1960). A combination of these effects and others might further increase the complexity of this seasonal fallout phenomenon.

At the present time, no quantitative information is available as to which process (if either) is the predominate cause of this seasonal fallout oscillation. This suggested examination of the cyclogenetic activity around the globe should provide some insight. Preliminary results of index calculations over a more extended period of time and a comparison with seasonal and global fallout data are forthcoming.

REFERENCES

Gustafson, P. F., S. S. Brar, and M. A. Kerrigan, 1961: Appearance of a spring maximum in nuclear test debris in 1960, Science, 133, 460-461.

Libby, W. F., 1959: Radioactive fallout particularly from the Russian October series, Science, 45, 151.

_____, and C. E. Palmer, 1960: Stratospheric mixing from radioactive fallout, Journal of Geophysical Research, 67, 1389-1400.

Mahlman, J. D., 1964: Relation of stratospheric - tropospheric exchange mechanisms to surface radioactivity peaks, Technical Paper No. 58, Department of Atmospheric Science, Colorado State University.

Miyake, Y., K. Saruhashi, Y. Katsurage, and T. Kanazawa, 1962: Seasonal variation of radioactive fallout, Journal of Geophysical Research, 67, 189-193.

Peirson, D. H., 1963: Beryllium-7 in air and rain, Journal of Geophysical Research, 68, 3831-3832.

Reiter, E. R. and J. D. Mahlman, 1964: Heavy fallout over southern United States in November

1962, Technical Paper No. 58, Department of Atmospheric Science, Colorado State University.

Staley, D. O., 1960: Evaluation of potential-vorticity changes near the tropopause and the related vertical motions, vertical advection of vorticity, and the transfer of radioactive debris from stratosphere to troposphere, Journal of Meteorology, 17, 591-620.

_____, 1962: On the mechanism of mass and radioactivity transport from stratosphere to troposphere, Journal of the Atmospheric Sciences, 19, 450-467.

Storebø, P. B., 1959: Orographical and climatological influences on deposition of nuclear-bomb debris, Journal of Meteorology, 16, 600-608.

_____, 1960: The exchange of air between the stratosphere and troposphere, Journal of Meteorology, 19, 547-553.